

1 "Supersessioning": A 2 hardware/software system for 3 electrophysiology spanning multiple 4 sessions in marmosets

5 Jens-Oliver Muthmann^{1*}, Aaron J. Levi¹, Hayden C. Carney¹, Alexander C. Huk^{1*}

*For correspondence:

huk@utexas.edu (ACH);

ollimuh@utexas.edu (JOM)

6 ¹The University of Texas at Austin

7

8 **Abstract** We introduce a straightforward, robust method for recording and analyzing spiking
9 activity over timeframes longer than a single session, with primary application to the marmoset
10 (*Callithrix jacchus*). Although in theory the marmoset's smooth brain allows for broad deployment
11 of powerful tools in primate cortex, in practice marmosets do not typically engage in long
12 experimental sessions akin to rhesus monkeys. This potentially limits their value for detailed,
13 quantitative neurophysiological study. Here we describe chronically-implanted arrays with a 3D
14 arrangement of electrodes yielding stable single and multi- unit responses, and an analytic
15 method for creating "supersessions" combining that array data across multiple experiments. We
16 could match units across different recording sessions over several weeks, demonstrating the
17 feasibility of pooling data over sessions. This could be a key tool for extending the viability of
18 marmosets for dissecting neural computations in primate cortex.

19

20 Introduction

21 The marmoset has drawn attention as a complementary nonhuman primate model system for vi-
22 sual neuroscience. While the dominant primate model system in neuroscience, the rhesus monkey
23 (*Macaca mulatta*), has the advantage of (relatively) rich cognitive abilities, a large body and robust
24 physiology, and an aggressive work ethic, their large and convoluted (gyrified) brains currently limit
25 the number of techniques that can be applied for measurements of neural activity. Thus, despite
26 their excellent trainability for complex tasks and willingness to engage in lengthy experimental
27 sessions, the scale and variety of neurophysiological questions that can be addressed have been
28 somewhat limited by practical constraints. Recently, the common marmoset (*Callithrix jacchus*) has
29 emerged as a complementary primate model system because of their smooth (lissencephalic) cor-
30 tex, opening up a much larger number cortical areas to the use of large-scale chronically implanted
31 electrode arrays (in addition to other techniques). However, a major current concern for adopt-
32 ing the awake behaving marmoset for detailed quantitative studies is their tendency to perform
33 far fewer trials per session compared to macaques. Such a behavioral limitation would result in
34 correspondingly smaller amounts of neural data (and hence, statistical power) per experiment, un-
35 dercutting the other advantages of the species, and likely limiting their applicability as a powerful
36 neurophysiological complement to the sorts of quantitative neuroscience work done in macaques.

37 To redress this fundamental potential limitation, we have developed a straightforward, user-
38 friendly tool for recording from large-scale arrays in marmosets while surmounting the relatively
39 short behavioral sessions performed by this smaller (and gentler) species. First, we report success-

40 ful long-term electrophysiological recordings using a new type of multi-electrode array for which
41 primate use has not yet been reported in publication to our knowledge, but which is commercially
42 available. These "3D" arrays are available with customizable electrode spacing not just across a
43 2D grid, but also along the depth of individual shanks. The arrays yielded good quality single-
44 unit (SUA) and multi-unit (MUA) activity, as demonstrated in two different marmoset cortical areas
45 (area MT, and the posterior parietal cortex, PPC). Second, we introduce a transparent means for
46 identifying activity recorded on these arrays, not just within individual sessions, but — importantly
47 — *across* sessions. This integration of hardware and software solutions allowed for data from the
48 same unit to be combined over multiple behavioral sessions, into what we termed "supersessions."
49 This brings the statistical power of awake-behaving marmoset neurophysiology closer to that of
50 macaques on a per-unit basis, while still allowing for larger scale recordings and/or powerful com-
51plementary tools that are more challenging to perform in macaques.

52 Here, we describe both the physiological and computational components of this tool and demon-
53strate its potential usefulness for transcending the behavioral limitations of marmosets into the
54realm of detailed, quantitative assessments of neural activity at large scales. Furthermore, the tool
55we introduce here is intentionally straightforward, meaning it can be readily implemented by oth-
56ers, as well as extended when ongoing updates to hardware and software emerge. We conclude
57by describing current limitations and how updates to this tool could further improve it.

58 To provide a bit more detail before delving into the results, we found that implanting commercially-
59available 3D "N-form arrays" (Modular Bionics) resulted in high quality, stable unit activity in mar-
60mosets. In our hands and experiences, this reflected a significant step forward in neural recording
61success, as prior attempts using more common types of 2D planar arrays (Utah, Black rock sys-
62tems) yielded less reliable and lower-quality outcomes. Although our goal was simply to record
63neural activity and not to mechanistically understand why a particular array style works better or
64worse, our hypothesis is that the slow insertion style (*Nicolelis et al., 2003*) and sufficient spac-
65ing between shanks of the N-form array (compared to *Rennaker et al. (2005); Karumbaiah et al.*
66*(2013)*), produces less damage, inflammation, and/or gliosis, and still reduces chronic respiratory
67micromotion. (*Prodanov and Delbeke, 2016*).

68 Given the success of the neural recording hardware in yielding qualitatively impressive neu-
69ral activity over long time periods, we designed a method to systematically compare and match
70(distributions of) spike waveforms across sessions. Our method identifies units from individual
71sessions independently, and then integrates spike clusters from new recordings into known, exist-
72ing ones identified in prior sessions. Analyses of units can therefore be performed over multiple
73experimental sessions.

74 In order to achieve a representation of spike shapes that was robust to potentially varying noise
75levels and/or forms across experimental sessions, we extracted simple properties of spike shapes
76in a narrow window around their peak. This was achieved by matching a family of predefined tem-
77plates on a GPU to yield a parametric representation of local excursions in the raw voltage traces,
78which included conventional unit spiking activity, spike events from weaker or more distant neu-
79ral sources, and noise. Unit isolation was not a conventional detection problem, and was instead
80transformed into a multivariate classification problem to be solved by a clustering algorithm. The
81resulting clusters were then matched across recording sessions. Although we are not deeply at-
82tached to this particular spike sorting approach, we provide it as a robust, intuitive starting point,
83which we validated against a more sophisticated and complex spike-sorting package. Its simplic-
84ity also allows for online views of sorting results during experiments, which could be useful for
85experimental decisions even if more sophisticated sorting routines are employed post hoc.

86 Taken together, this work puts forth a synthesis of commercially-available hardware and intu-
87itive software that allows experimenters to overcome one of the major limitations of the marmoset
88as a model species by introducing the concept of supersessions. More generally, this framework
89may support better integration of work done in marmosets and macaques, allowing these two
90awake-behaving primate preparations to have greater scientific overlap and thus to more solidly

91 allow for their relative strengths and weaknesses to be considered.

92 **Results**

93 **Neural activity apparent for more than 9 months on chronically-implanted 3D ar-** 94 **rays**

95 We recorded single and multi-unit (hereafter, "unit") activity in the brains of 2 marmosets, one with
96 a 3D N-form array in and around the middle temporal area (MT), the other with an identical array
97 placed in posterior parietal cortex (PPC). For both arrays (Figure 1 A, B, respectively), we were able
98 to record spiking activity starting a week after insertion. Activity lasted for a duration of at least
99 9 months, as depicted in Figure 1 (top rows). Figure 1 (second rows) show, in comparison, the
100 relatively short durations of individual recording sessions (approximately a half hour to an hour).
101 These durations likely reflect a lower bound on how long marmosets will work, as they were largely
102 determined by the animal's preponent motivation to engage in various visual tasks with no fluid
103 or food restriction.

104 Signal amplitudes (Figure 1, third rows) were fairly constant over long periods of time, per-
105 haps with the first two weeks after implantation yielding smaller signals before stabilizing (i.e., first
106 few recording sessions, visible at the very left of the plots). A gradual decline in signal amplitude
107 was further apparent after about 7 months for marmoset J. Detected events (see Methods) had a
108 wide amplitude range of relatively sparse (0.1 – 10 Hz) events, indicative of spiking activity (Figure
109 1, bottom rows). Taken together, these descriptions of the behavior of the animals and the signals
110 from the electrode arrays lay the groundwork for attempting to stitch together data from multiple,
111 subsequent recording sessions. The next critical step would be identifying unit activity that could
112 conservatively be identified across such sessions.

113 **Spike clusters overlap in consecutive sessions**

114 Our goal was to identify spikes from the same units across recording sessions. This required mea-
115 sures that would be robust to noise, in the sense that spikes from other neurons would not perturb
116 or distort characterization and identification of a given unit. To that aim, we focused our analysis
117 on a very short temporal window, including only the depolarization phase of a spike, represented
118 by a local minimum in the raw voltage traces.

119 For each local minimum (i.e., putative spike) in the raw voltage trace, we determined: (a) ampli-
120 tude, measured as the dot product with a template (of unit power), expressed in standard devia-
121 tions (σ), as calculated on the high-pass filtered voltage traces; (b) width, measured as the full width
122 at half minimum; and (c) symmetry, measured as the ratio of its falling and rising phase durations
123 (i.e., a 1 : 2 ratio means that recovering back to baseline took twice as long as reaching the voltage
124 minimum).

125 These parameterized shape characterizations of the units were put into 3D-histograms (marginals
126 shown in Figure 2 A) for each recording session, and clustered using a watershed algorithm (see
127 Methods for details). This procedure yielded shape clusters (cyan markers in Figure 2 A) for every
128 session in a common coordinate system to allow for cross-session comparisons of spike shapes.
129 Shape clusters between consecutive sessions often looked very similar, and so we further tested
130 whether they likely reflected spikes from the same or from different units.

131 Specifically, if the brain tissue was held in place by the 16 electrode shanks of the array such
132 that relative movements between the electrodes and the sampled neurons rarely happened, we
133 would always record from the same neurons and see identical spike shapes. Otherwise, if there
134 were substantial shifts in relative position between brain and electrodes, both amplitude and spike
135 shape would shift with movement, and we would be unable to track units across a large number
136 of sessions.

137 We were indeed able to systematically match units across recordings. This was done quantita-
138 tively, using the Jensen-Shannon divergence as a distance measure in the histogram shape space

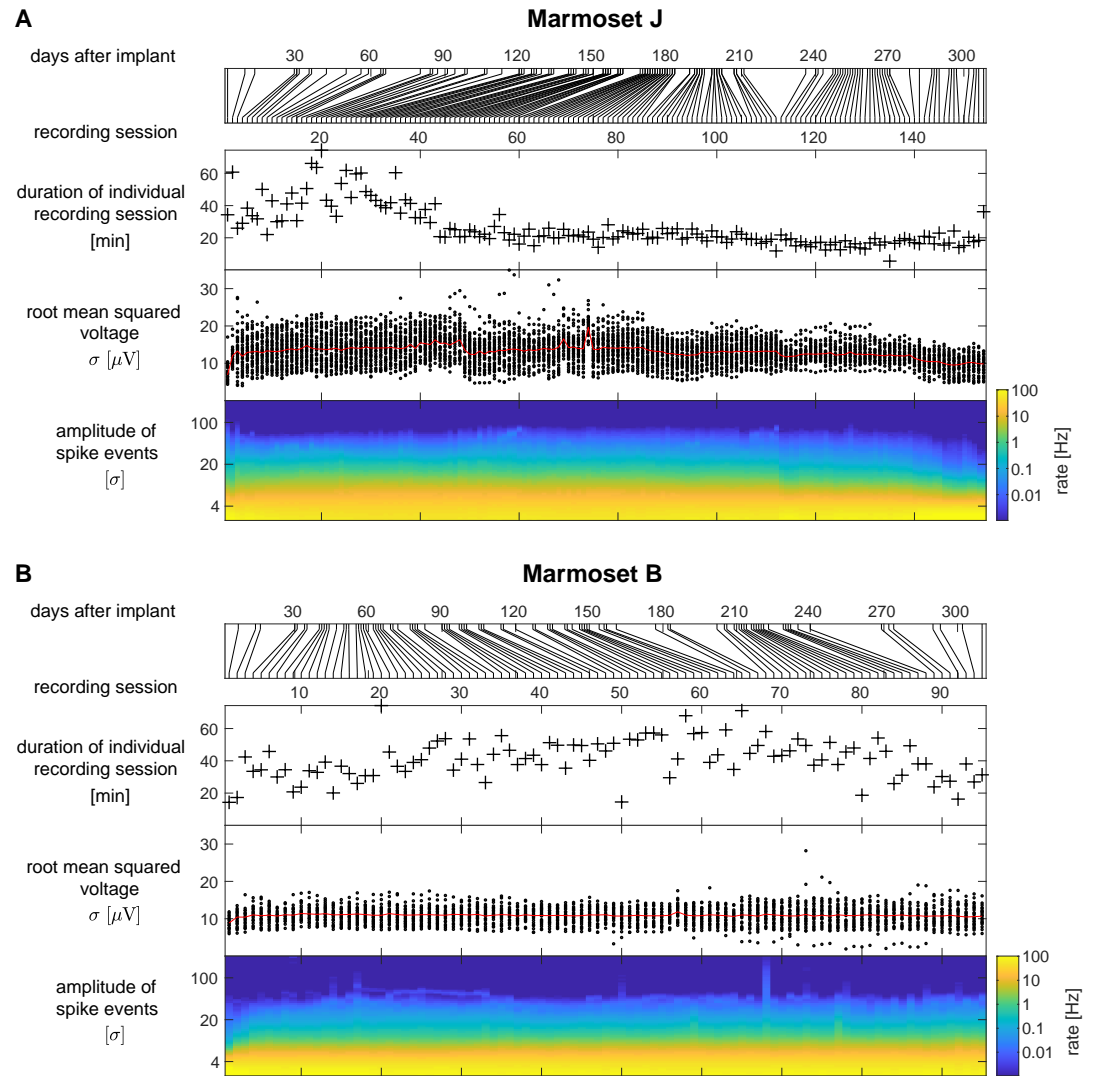


Figure 1. Long-term stability of arrays. **(A)** Marmoset J. Top panel: Illustration when individual recording sessions were performed. For clarity, the plots below and in subsequent Figures reflect individual recording sessions rather than time. Second row: Durations of electrophysiological recordings in individual sessions. Third row: Root-mean-squared voltage fluctuations of the common averaged, 300 Hz high-pass filtered data (scatter plots for active electrodes, average shown in red). Bottom row: Amplitude histograms of detected events, averaged across electrodes. **(B)** Same statistics for Marmoset B.

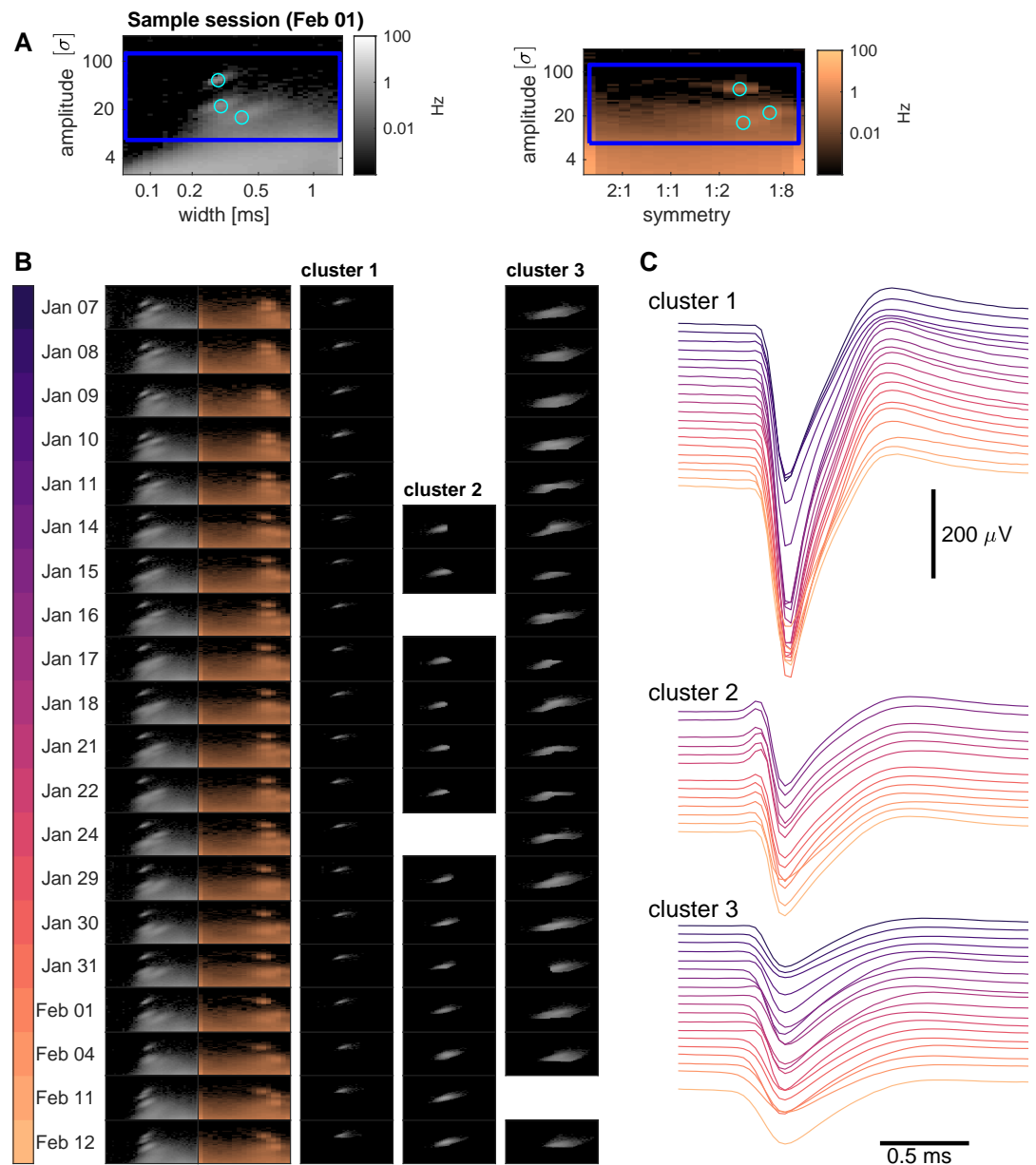


Figure 2. Example of merging clusters across sessions. **(A)** Histograms for amplitudes and widths (left panel) or symmetries (right panel) of detected events on February 1. Regions outlined in blue are shown for a range of dates in (B), using the same color code and axes. Cyan circles mark the three clusters detected in this session. **(B)** Left: marginal histograms of local maxima for 20 consecutive recording sessions, labeled with dates. Right: temporal matches of the 3 clusters found on February 1. **(C)** Waterfall plots of average spike shapes, for dates as color-coded in (B). Data from marmoset B.

139 (allowing for small amplitude shifts under a penalty). Figure 2 B shows an example of tracking the 3
140 units observed on February 1 across multiple sessions. Cluster 1 provides an example of a clearly
141 isolated unit with very large spikes, which lasted for about 5 weeks. For this cluster, averaged spike
142 shapes were very similar across recording sessions, with smaller amplitudes for the initial and fi-
143 nal recordings (Figure 2 C, cluster 1). Cluster 2 represents a cluster with decent amplitude spikes
144 but relatively common spike shapes, resulting in highly variable sorting performance. While being
145 reasonably well isolated from January 29 to February 1, it is contaminated to a variable degree
146 with spikes from different units in other sessions and couldn't be separated from another cluster
147 in two intermediate recording sessions. Cluster 3 had low spike amplitudes, but would be con-
148 sidered a decent multi-unit cluster from January 29 to February 1. For the other sessions there is
149 a small local maximum in the shape histograms, but the cluster would be considerably contami-
150 nated with unclassified, smaller amplitude spikes. Given that larger amplitude clusters slowly (and
151 independently) drift over time, we can assume that the same happens to units in this cluster, mak-
152 ing it difficult to obtain exact matches across recordings. But, the relatively moderate firing rate of
153 the cluster would suggest that few units with defined shapes were involved, distinguishing it from
154 unclassified spikes.

155 In conclusion, our main result is that matching simple shape statistics of spike waveforms across
156 several recording sessions using N-form arrays in marmosets is feasible, and for some units this
157 consecutive recording is possible over notably long periods of time (> 1 month). This grants us the
158 capacity to combine data from multiple experimental days, which we deem "supersessions".

159 **Tuning properties on individual electrodes are stable across sessions**

160 We further confirmed the stability of the measured "supersession" neuronal activity by evaluating
161 the cross-session consistency of physiological tuning properties. This evaluation was done for the
162 MT array implanted in marmoset J, where we were able to confirm that several sites on the array
163 showed directionally-tuned activity in response to moving dots in the left visual field (as expected
164 when recording from area MT in the right hemisphere).

165 The MT electrodes recorded strongly tuned multi-unit activity, so we focused on MUA super-
166 sessions for this analysis. We again used our parameterized representation of spike shapes to
167 determine a region of interest (Figure 3 A, E, outlined in black) in spike shape space with strong
168 directional tuning across recording sessions (Figure 3 A, E). This was feasible because tuning on a
169 given electrode was consistent across a wide range of spike shapes (Figure 3 B, F). For the two MUA
170 sites shown as examples, the direction tuning curves measured were stable over almost 3 weeks.
171 This stability of physiological properties, built on top of the stability of spike shapes themselves,
172 further strengthens the case for the validity and viability of supersessions.

173 We therefore created supersessions across these sessions that exhibited stable tuning and
174 spike shapes, which allowed us to combine larger amounts of data for a single analysis. As an ex-
175 ample here, we show that supersessions allow us to resolve the detailed time course of responses
176 to individual motion directions at a high temporal resolution (Figure 3 C, G). Note that transient
177 aspects of the motion-driven response were very short and consisted of only a few spikes per trial,
178 such that averages across many trials were beneficial. To illustrate this effect, we show the same
179 analysis for responses obtained in a single session (Figure 3 I-K). Averaging over the temporal re-
180 sponses, we then obtained tuning curves for individual sessions (Figure 3 D, H, L).

181 In this example, tuning was stable for considerably longer than one week. This demonstrates
182 that not only were shape clusters with high amplitudes were stable across sessions, but also that
183 functional properties of low-amplitude activity were conserved across many sessions. Further-
184 more, being able to combine 10 or more sessions provides an order-of-magnitude increase in trial
185 count that, even assuming some degree of lower-quality unit isolation, should counterweight the
186 relatively short individual behavioral sessions. We delve into this issue in more depth at the end
187 of the results sections.

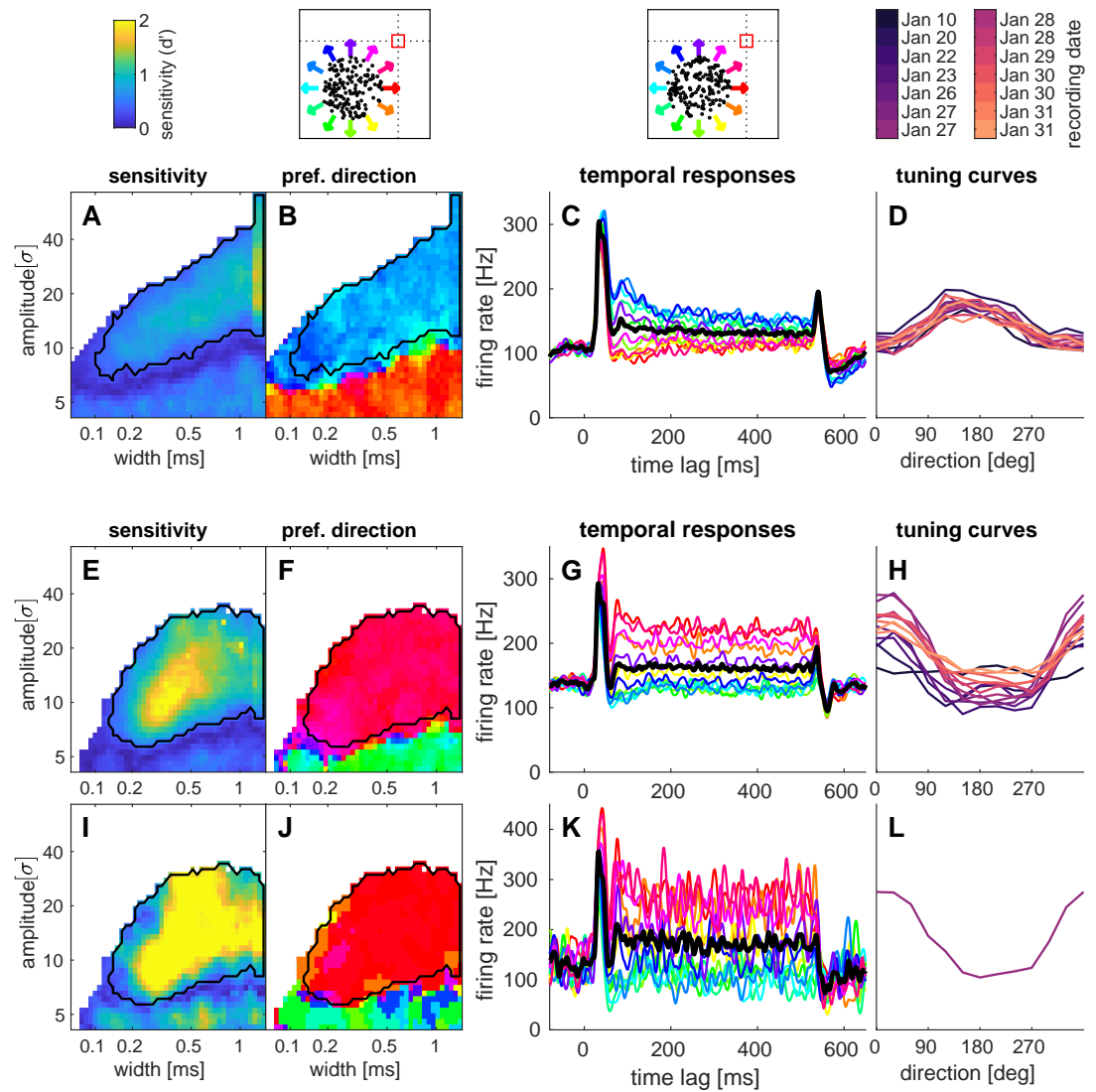


Figure 3. Examples of direction tuning on two electrodes. Top: Legends and stimuli for the examples below. Moving dots were presented at (-15,-15) degrees from the fixation point (red square). (A) Sensitivity indices and (B) maximum response directions in dependence of spike shapes. (across sessions, corrected for a cross session baseline effect). The region outlined in black was used for further analysis. (C) Temporal firing rate responses, averaged across sessions and shown for individual tuning directions (colored lines, black line: avg. response, 4041 trials). (D) Tuning curves obtained for individual recording sessions (labeled above, some dates had a morning and afternoon session). (E - H) Same analysis for a second example electrode. (I - L) Tuning observed in a single session (January 27 afternoon session, 254 trials). Recordings in area MT (marmoset J).

188 **Most units in a given recording were observed for several sessions**

189 Having established stability of both spike waveforms and physiological tuning, we now turn to
190 report a more comprehensive statistical description of recording stability and our ability to distin-
191 guish spike shape clusters (i.e., to isolate one unit from another). A summary of all tracked units
192 across recording sessions is shown in Figure 4. Spike clusters were regions in 3D-shape-histograms,
193 consisting of a set of voxels, which could be divided into boundary voxels (adjacent to a voxel out-
194 side the cluster) and center voxels. If the average spike count in boundary voxels was less than 3/4
195 of the average density in center voxels, clusters were considered as "better-isolated" and shown
196 in darker colors in Figure 4.

197 We further distinguished clusters that lasted for shorter numbers of sessions (<5 , orange) and
198 longer numbers of sessions (blue, ≥ 5), as many of the short-lived units had low amplitudes and
199 were less reliably detected. We found that a large proportion of units in a given recording survived
200 for multiple recording sessions (histograms in Figure 4, blue vs. orange), especially when they were
201 considered as better-isolated (Figure 4, darker colors).

202 A more detailed visualization of the survival of individual units is shown in the upper half of
203 both panels in Figure 4. This plot can resolve whether the appearance or disappearance of units
204 between two sessions happened locally (i.e., affecting only some individual units), or globally (i.e.,
205 affecting most, if not all, units across the array). To further see whether the temporal separation
206 (i.e., number of days) between consecutive sessions was a major factor for the loss (turnover) of
207 units, we visualized the relation between the number of long lasting units lost and the temporal
208 separation between the two sessions when the loss occurred (Figure 4, insets). Although larger
209 temporal separations tended to correlate with a higher turnover of units, substantial unit turnover
210 could also occur even with very short temporal separations between sessions.

211 This analysis also highlights a difference between the two animals: while there are several dis-
212 tinct time points of high turnover in marmoset J (Figure 4 A, likely indicative of discrete changes in
213 electrode array position), no such events could be identified in marmoset B (Figure 4 B, likely in-
214 dicative of only smaller and/or more gradual changes in array position within the brain). Although
215 we are not sure why the array stability was different in the two animals, this does show that: (a) our
216 analysis scheme is capable of revealing changes and differences in stability; and (b) regardless of
217 whether an array was stable over longer or short terms with or without distinct temporal changes,
218 it is possible to follow units across supersessions in both regimes.

219 Figure 5 shows descriptive histograms of the basic properties of all detected shape clusters
220 (grayscale background). We distinguished clusters that survived short-term (upper row) and long-
221 term (lower row). Several basic relations become apparent from visual inspection. First, the spread
222 (avg. diameter) and firing rates of clusters tended to be larger for smaller amplitude waveforms,
223 likely reflecting the effects of merging overlapping shapes from multiple units. Second, large am-
224 plitude waveforms were generally more skewed than those with low amplitudes, likely reflecting
225 our descriptive approach's ability to identify the basic shape of individual unit waveforms. Third,
226 waveforms from the array in MT tended to be narrower than those from the PPC array, perhaps
227 revealing a biophysical difference that our approach is capable of picking up.

228 Viewing these basic descriptive plots, we also wondered whether long term matches of spike
229 clusters might be a result of detecting different units that just happen to produce similar shapes.
230 To test this, we estimated how likely a given cluster might be mistaken for a different cluster by
231 counting the clusters with similar spike shapes from all recording sessions. We then ranked better-
232 isolated clusters according to the number of similar shaped clusters. The resulting rank a cluster
233 had in the sorted array is depicted in color in Figure 5. A low rank corresponds to isolated units and
234 a low likelihood to detect the same cluster by chance (Figure 5, yellow/green circles), and a high
235 rank means that the corresponding spike shapes were frequently observed (Figure 5, blue circles).

236 Sorting clusters in this way allows us to investigate whether clusters with commonly observed
237 spike shapes would show a bias in long-term survival. We observed that many clusters with unique

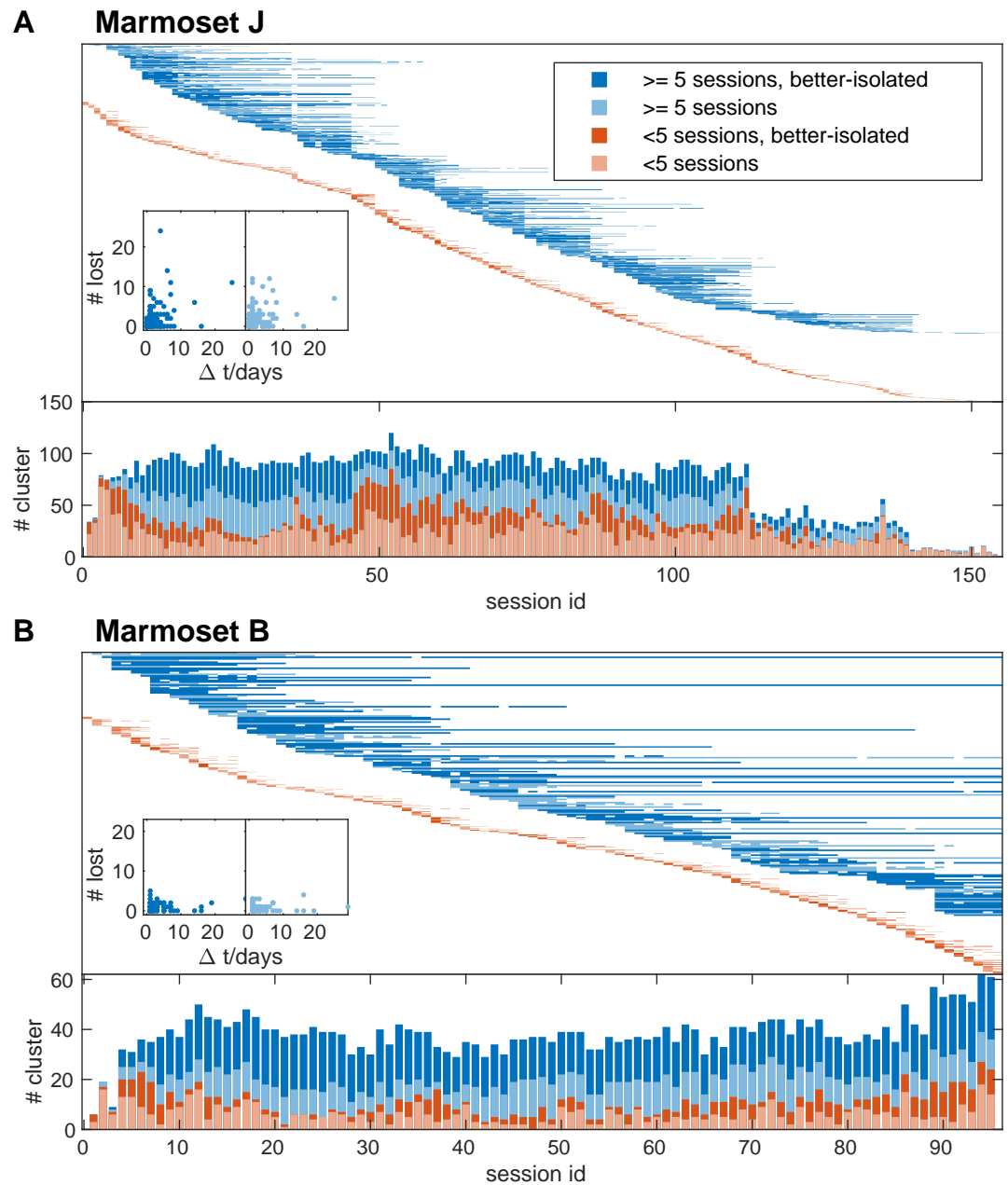


Figure 4. The majority of clusters survives for multiple sessions. **(A)** Clusters detected in recordings of area MT (marmoset J). Top: temporal pattern of long-term (at least 5 sessions, blue) and short lived (<5 sessions, orange) clusters. Better-isolated clusters are shown in darker shades. Inset: Number of disappearing units in dependence of the temporal gap between two recording sessions. Bottom: Number of clusters in each session. **(B)** Same plots for recordings in PPC (marmoset B).

238 shapes survived less than 5 sessions (Figure 5, yellow circles). However, we also noticed that many
239 of these clusters had relatively low amplitudes and therefore might have been lost, not due to
240 actual changes in the presence of the unit over a particular (brief) time frame, but due to insuffi-
241 cient signal-to-noise ratio relative to our spike-identification standards. We therefore re-focused
242 our analysis of the relation between spike waveform uniqueness and lifetime using only clusters
243 surviving for at least 5 sessions.

244 In order to assess whether clusters with more or less common waveform shapes might show

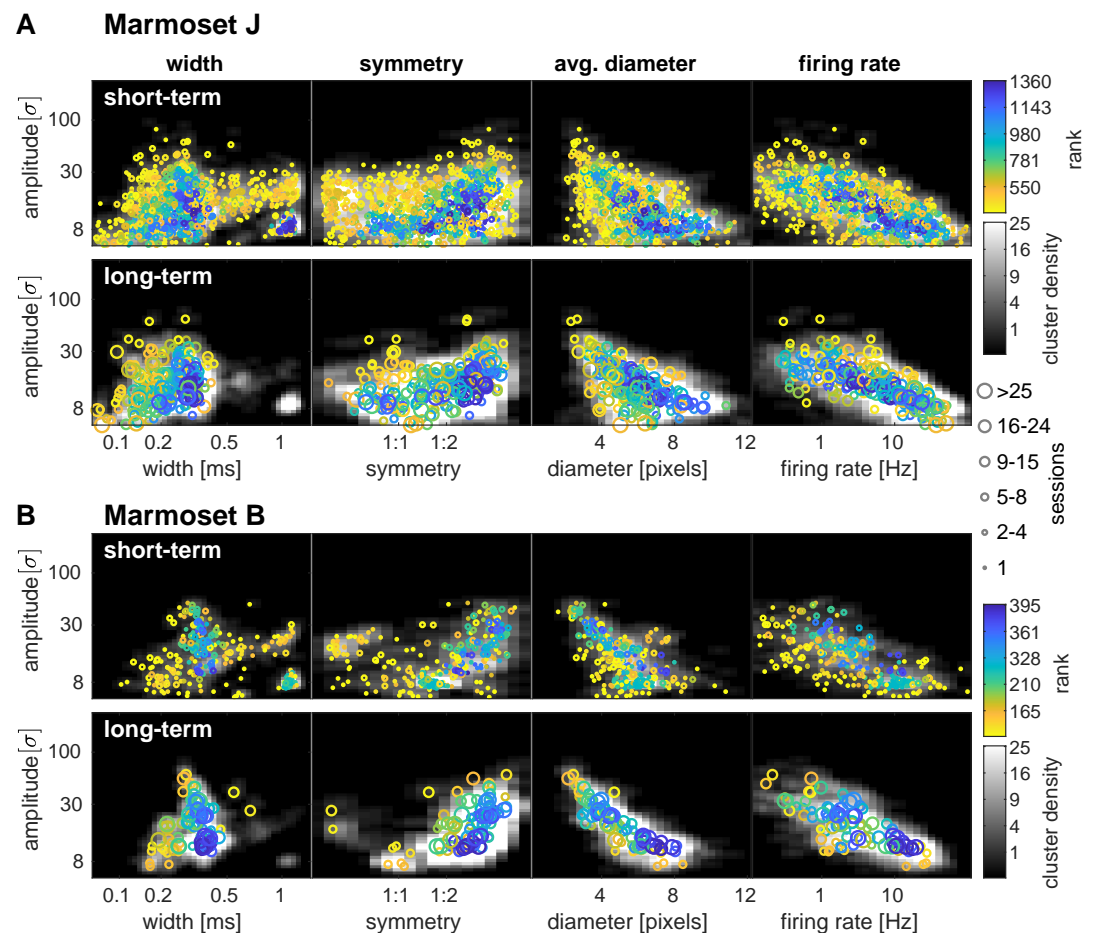


Figure 5. Detected shape clusters are similar (at a population level) when observed for multiple sessions. **(A)** Clusters detected in all recordings and electrodes of area MT (marmoset J). Grayscale represents the density of all detected clusters without merging them across sessions. Colored circles represent individual, better-isolated clusters, merged across sessions. These were ranked according to the corresponding overall density of clusters (i.e. grayscale background) and this ranking is shown in color. Specifically, properties of clusters depicted in yellow were rarely observed and those in blue were commonly found in the data. Clusters surviving less than (top row) and at least (bottom row) 5 sessions are plotted separately for clarity. **(B)** Same analysis for recordings in PPC (marmoset B).

245 a difference in their lifespans, we analyzed cluster survival, excluding different amounts of the
 246 most common cluster shapes. Due to the limited amount of data, we visualized the inverse of
 247 the expected lifetime at a given age, which is assuming a constant probability to lose a cluster in
 248 each session. Figure 6 shows that this assumption is reasonable, as the fraction of clusters lost per
 249 session does not change dramatically after 5 sessions. Importantly, except for clusters with the
 250 10% most uncommon shapes, the rate at which spike clusters were lost over time did not depend
 251 on how common the spike shapes of that cluster were. This is good news, as it does not appear that
 252 the longevity of units over sessions is strongly confounded by the appearance and disappearance
 253 of units which happen to have similar spike shapes.

254 This analysis also revealed an interesting difference between the two animals: For the array in
 255 PPC, cluster survival was about twice as long as for the array in area MT. Although there were more
 256 clusters observed for the MT array, we also observed greater variations in signal amplitude and we
 257 gradually lost signal in the later recordings of that array (Figure 1 A). We therefore infer that the
 258 observed effect could have been due to a higher degree of general instability of the MT array over

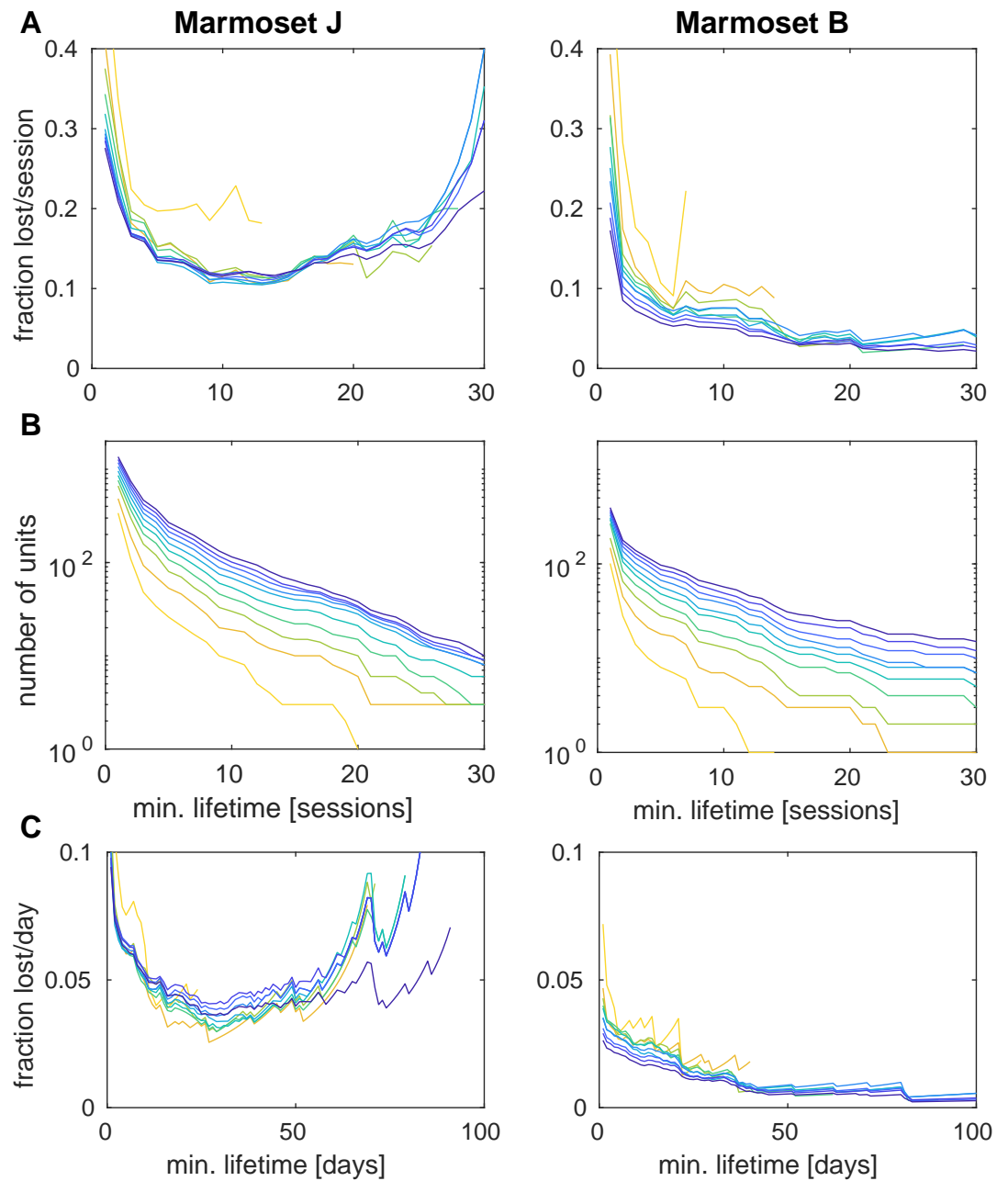


Figure 6. Cluster survival is not an effect of common spike shapes. **(A)** Estimated fraction of the clusters that would be lost after surviving the number of sessions indicated on the x-axis. Coloured lines correspond to the fraction of clusters included in the analysis (steps of 10%, as in Figure 5), where the most yellow curve corresponds to only including the 10% most uncommon shapes. **(B)** Number of units observed for a minimum lifetime. **(C)** Same as in (A) when measured in days rather than sessions. Recordings in area MT (marmoset J, left column) and PPC (marmoset B, right column).

259 time.

260 **Supersessions provide the power to estimate spatial and temporal aspects of re-**
 261 **sponses across sessions**

262 Finally, we tested whether clearly isolated units could be matched across multiple sessions to as-
 263 sess their spatial and temporal properties. We therefore performed generic receptive field map-

264 ping assays at regular intervals over multiple experimental sessions. As proof of concept, here, we
265 describe an example in which both spatial receptive fields and temporal dynamics of responses
266 were estimated using supersession data.

267 Figure 7 shows two example units. The first unit had well isolated, high amplitude spike shapes
268 (Figure 7 C,E) and a pronounced refractory period (Figure 7 F) for at least 6 recording sessions (fir-
269 ing rate (1.7 ± 0.2) Hz; avg. spike count per trial (400 ms) 0.7 ± 0.4 overall and 1.5 ± 0.5 for stimuli in
270 the receptive field). It consistently responded transiently to stimuli in the left visual field, 50-80 ms
271 after stimulus onset. The second example ((Figure 7 G-L) shows a unit with an amplitude gradu-
272 ally increasing and decreasing across sessions. Corresponding to an increase in SNR and lower
273 contamination by false detections averaged spike shapes became sharper for sessions with large
274 spikes (Figure 7 K). This unit had a much faster response around 40 ms, consisting of about 1 spike
275 per trial (and eventually a slightly elevated sustained activity during stimulus presentation). In both
276 of these cases, the response properties of the unit would have been difficult to determine using
277 only a single session's worth of data, due to the low absolute number of spikes recorded. For ex-
278 ample, the total number of spikes recorded in the first 400 ms in the receptive field of the unit in
279 a single session was just 20-80 spikes, the total number of spikes across all trials about twice that
280 amount. But by evaluating data across sessions, the supersession data shows that these units had
281 clearly-localized receptive fields.

282 Discussion

283 Modern neurophysiological studies in primates require increasingly large amounts of data, either
284 because the parameter space of relevant stimuli or behaviors grows richer (and hence, data are
285 distributed across a larger number of conditions), or because the goal of the experiment itself
286 is to measure more detailed aspects of population activity (and hence, more data are required
287 to estimate higher order statistics). Here, we established the potential of chronically-implanted
288 3D electrode arrays, coupled with a simple unit identification scheme, to allow for the creation of
289 supersession datasets that transcend the standard limitations of marmoset behavior within indi-
290 vidual experimental sessions. We found that high quality activity was evident on this type of array
291 for many months, that a mixture of stable SUA and MUA data could be collected spanning multi-
292 ple individual sessions, and that these supersessions yielded stable physiological characterizations
293 that were more detailed than those from single sessions.

294 Recording performance

295 With the goal of making the marmoset more strongly viable for detailed quantitative studies, we
296 aimed to develop an analysis pipeline that would be robust to different levels of recording quality,
297 measuring single-unit activity where possible, but at the same time considering multi-unit activity.
298 When applying this analysis to data recorded from implanted electrode arrays over the course of
299 more than 9 months and averaging across all recording sessions, we obtained 28 better-isolated
300 units/array/session. For individual arrays, these averages were 32 and 23 for marmoset J and B,
301 respectively, 20 and 18 of which would be seen across a span of five or more sessions. In addi-
302 tion, we found another 40 and 16 multi-unit clusters per array per session for marmosets J and B,
303 respectively; 18 and 10 sessions lasting for five sessions or more).

304 In comparison, previous reports of recording stability using planar (2D) 'Utah' arrays in macaques
305 (*Dickey et al., 2009; Vaidya et al., 2014; Fraser and Schwartz, 2011*) focused on single unit activity,
306 which strengthened their claims to be able to track individual units, but at the cost of discarding
307 multi-unit activity. Values reported in those prior studies were at most 137 units/array/session, but
308 with large variations across arrays and with decreasing number over time, the average values were
309 closer to 30 units/array/session. In addition, most recordings were done in the first two months
310 after implantation, possibly implying a quicker falloff in signal quality than we encountered with
311 different arrays, and making the comparison to our unit identification and quality less direct.

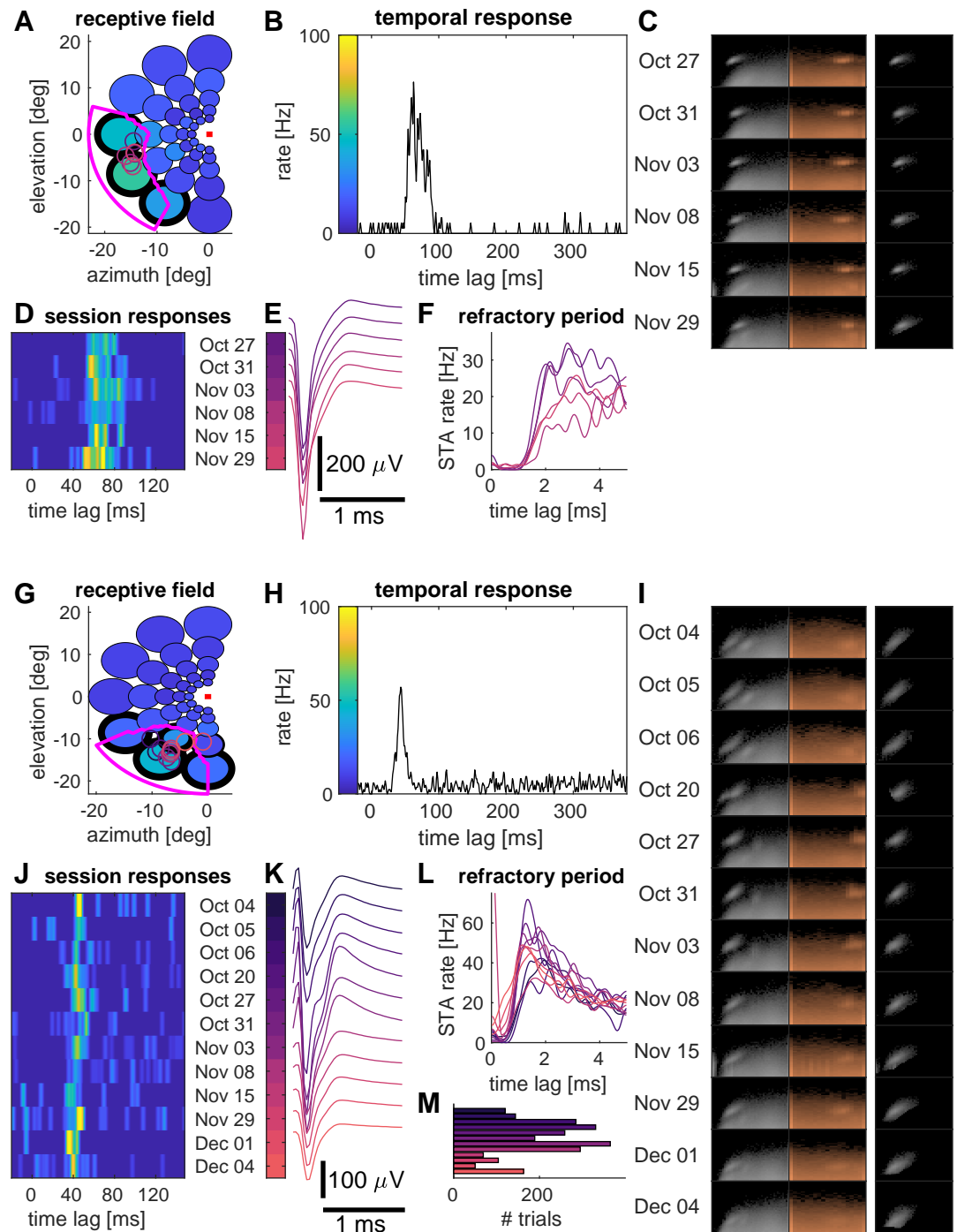


Figure 7. Examples of receptive fields of two units near area MT. **(A)** Maximum firing rates in response to presentation of a disk of moving dots (diameter scaled by 1/2 for clarity; colors indicates firing rate) at a given location in the visual field (fixation spot indicated by a red square). The receptive field (region where the interpolated firing rate exceeded a threshold; see Methods) is outlined in magenta. Colored circles represent estimates of receptive field locations for individual recording sessions. **(B)** Average firing rate for the three conditions (around the RF) outlined in black in **(A)**. **(C)** Marginal shape histograms (as in Figure 2). **(D)** Close-up for firing rates shown in **(B)** for each recording session. **(E)** Averaged spike shapes. **(F)** Spike triggered averaged firing rates show a refractory period after spikes. **(G-L)** Same as **(A-F)** for a different unit. **(M)** Total number of trials per session. Colors indicate recording dates (sessions) and firing rates, respectively, and are matched across panels. Recordings near area MT (marmoset J).

312 Although a complete comparison between these types of array is beyond the scope of this
313 proof-of-concept tool introduction, we believe it is likely that the variations in performance ob-
314 served with 'Utah' arrays in macaques were larger than for the 3D arrays we used. In fact, in mar-
315 mosets, arrays with similar sizes as the ones used in this study (but with fewer electrode contacts)
316 have been reliably implanted and often measured spiking activity for months (*Debnath et al., 2018*).

317 We conclude this comparison by noting that we recorded from a similar number of units as
318 reported for the larger 96 channel 'Utah' arrays (*Dickey et al., 2009; Vaidya et al., 2014; Fraser and*
319 *Schwartz, 2011*), but from a smaller region of the brain, largely thanks to the denser 3D geometry
320 of the arrays. This is another advantage on the hardware side of this tool, as it allows for larger
321 scale recordings within small brain areas in the marmoset- arrays built for larger primate brains
322 will often sparsely sample within a single area, spanning their footprint over many adjacent areas.

323 **Long-term stability of units**

324 The 3D array recordings had excellent long-term stability, which is a novel and important result for
325 studies using marmosets. The feasibility of long term recordings is itself not totally unprecedented,
326 as there are multiple approaches that align with our observations in a number of species. Here we
327 review some examples, not just to bolster the case that long term stable recordings can be made
328 in a number of species, but to point to the broader potential adoption of the supersession analysis
329 approach we have introduced.

330 For example, *Jackson and Fetz (2007)* used microwires and studied stability of single units in
331 continuous recordings using a window discriminator, and found single units surviving for up to
332 17 days in a one year experiment, where microwires were moved periodically to different neu-
333 rons to improve signal quality. More systematic experiments addressing long-term stability of in-
334 dividual units were done with 'Utah' arrays by matching spike waveforms and inter-spike interval
335 histograms across recording sessions (*Dickey et al., 2009; Vaidya et al., 2014*), eventually in combi-
336 nation with correlations and firing rates (*Fraser and Schwartz, 2011*) to increase statistical power.
337 While comprising relatively small numbers of units and recording sessions, these studies demon-
338 strated a few single units being recorded for months, suggesting that there was likely no relative
339 movement between the electrodes and the neural tissue. *Linderman et al. (2006)* used continu-
340 ous recordings were used to study short-term changes of spike amplitudes and reported moderate
341 amplitude fluctuations in two example units.

342 The N-form arrays we used had the same spacing between shanks as the 'Utah' type of array
343 — albeit with a higher density of recording sites along a shank, and far fewer total shanks. Even
344 though the N-form arrays comprised only 16 shanks, we found a similar long-term stability for
345 well-isolated single units, suggesting that this number of shanks is sufficient to mitigate substantial
346 array drift. The smaller "bed of nails" also permits a slow insertion method, which we hypothesize
347 is important for avoiding damage associated with ballistic insertion methods, especially important
348 in the smaller and more delicate marmoset brain.

349 In assessing the usefulness of supersession unit data, we used relatively relaxed criteria for unit
350 selection. Given this liberal approach, we did not focus on comparing session-scale average spike
351 waveforms (as these are sensitive to varying amounts of other-spike contamination and , but rather
352 distributions of a parametric representation of spikes, where contamination could be considered
353 as a mostly flat, additive component. Likewise, we dropped the comparison of inter-spike interval
354 histograms, firing rates and correlations. While these can provide useful information about unit
355 identity, they rely on a high SNR and good isolation of units in every single session and might even
356 depend on the animal's engagement in experiments. To avoid discarding large amounts of good
357 data without further inspection, we argue that these measures might best be used for post-hoc
358 tests. Spike shapes themselves proved to be reasonably informative about cluster identity, and
359 for short experimental sessions and low firing rates, multiple sessions may be required to obtain
360 useful second order estimates.

361 Recent studies in rodents have been very successful in long-term tracking of neuronal activ-

ity. However, this performance was in large part made possible by increasing the density of electrode contacts, and therefore the number of observables available for spike sorting. Specifically, *Okun et al. (2016)* successfully sorted concatenated data for a small number of sessions and immobile NeuroNexus silicon probes with 4-8 tetrodes (slow insertion). Tetrode recordings in mouse (*Dhawale et al., 2017*) have been used for continuous tracking over weeks. Continuous tracking seems required here due to larger fluctuations in electrical coupling of neurons to electrodes. Recent work with high density arrays (*Chung et al., 2019*) in rats showed smaller fluctuations and allowed sorting segments of data and linking these together. Other recent high-density recording techniques using ultraflexible mesh electronics (*Fu et al., 2016, 2017*) and silicon high-density arrays (*Jun et al., 2017b*) have not yet been systematically studied for unit longevity. In primates, heptodes have been used in acute recordings, in marmoset cerebellum (*Sedaghat-Nejad et al., 2019*) and in macaques *Kaneko et al. (2007)*, and single unit tracking was done in the latter case.

In terms of stability of units, the following general picture emerges: wires and tetrodes drift within days, but stability is better when they are left in place without an attached micromanipulator *Okun et al. (2016)* or when they are continuously tracked (*Dhawale et al., 2017*), approaches which can yield stability for days to weeks. Multiple shanks likely reduce electrode drift and units can be tracked for weeks to months ('Utah' arrays potentially for months if no degrading signal quality, *Vaidya et al. (2014); Fraser and Schwartz (2011)*), while ultraflexible, polymer based electrodes might remain stable even longer. Our results fit well into this picture.

Implications for experimental planning and spike sorting methods

Long-term stability offers the potential to generate detailed characterizations of neuronal behavior, but it also requires more careful experimental planning. In the two sections below, we highlight conceptual differences for experimental planning and spike sorting compared to the classical single-session approach.

Experimental Planning

While the general long-term stability and the observation of single- and multi-unit activity did support more data-rich analyses than would have been possible from a single session, the fashion in which units ended up being sampled across recordings crucially affects the planning of possible experiments. If, at one extreme, we had recorded from a different set of neurons in every recording session, we would have ended up with a large sample of recorded neurons, but not more data per unit. Such a scenario would be allowing us to estimate distributions of neuronal behavior in a given area. At the other extreme, if we were to always record from the same set of neurons, we would end up with a small sample, but would be able to measure their responses in many different conditions and further quantify the higher-order statistical interactions between them.

In reality, we found ourselves in a fruitful middle regime: Units were recorded for variable durations, in which a small fraction of units both appeared and was lost between recording sessions. This process was not entirely random, as we saw that most units disappeared during the initial sessions after their appearance. This means that the chance for a unit to survive for another session increased with the number of sessions that this neuron had already been observed. Hence, if we were to ask which of the units we would most likely observe in a future session, the best bet would be those units that were already observed for the most sessions in the past.

The variable lifetimes of units also provide an additional tool for raising the standard for isolation. Restricting an analysis to only long-lasting units would likely reduce the chance of including less clearly isolated units. Such units may not be found in some of the recordings due to variations in signal amplitude.

The exact timescales at which units were lost between sessions varied slightly across our two test arrays/animals. However, there may be two different mechanisms involved: while we found a relatively low, constant turnover of units on both arrays, in marmoset J we additionally saw a few events where a large fraction of units was lost between subsequent recordings (Figure 4). These

411 events could not be explained by a long temporal gap between the recordings, suggesting a rela-
412 tively fast mechanism for that, with a timescale of hours to days (as opposed to weeks and months).
413 We believe that these findings can impact the planning of experiments using chronic arrays.
414 In the classical single session approach, experimenters devote part of the experimental time for
415 general characterization of receptive fields and tuning of neurons, in order to target a neuron and
416 adapt the stimulus properties to efficiently sample responses, avoiding stimuli without an expected
417 effect on the neuron's firing behavior. In the case of chronic array recordings, we record from
418 many neurons with potentially different receptive fields and tuning properties, suggesting the use
419 of more general stimuli, e.g. sampling a larger visual area and different tuning directions. Especially
420 when studying interactions between a small number of units, one should keep in mind that some of
421 these units may disappear during the course of an experiment and it would be advisable to start
422 with a larger group of candidate units. In this regard, chronic arrays would be ideally suited for
423 continuous tasks and naturalistic stimuli (e.g. *Huk et al. (2018)*; *Knöll et al. (2018)*), which efficiently
424 sample a large parameter space, allowing for simultaneous characterization of units with different
425 tuning properties.

426 If, however, an experimental design requires finding persistent units in order to adapt focused
427 studies to suit their tuning, we recommend choosing units that have already been observed for
428 at least 3 sessions, as these units have a high chance to survive the next sessions. In our experi-
429 ments, such units had a conditional (additional) lifespan of 6 and 14 sessions (for marmoset J and
430 B, respectively, cf. Figure 6 A). Likewise, studies of changes in firing behaviour of single units across
431 sessions (e.g. while an animal is learning a task, or after drug treatment) are in principle feasible.
432 However, such experiments can usually not be repeated in the same animal, and few units will be
433 clearly isolatable, resulting in a rather inefficient use of the acquired data. In this case, the sug-
434 gested approach is to perform several consecutive studies on an animal, which is possible given
435 the longevity of the arrays used here.

436 Importantly, we have shown that it is feasible to combine data across multiple sessions to in-
437 fer tuning properties of neurons from multiple sessions. The same should be possible for inter-
438 neuronal correlations. Our results also highlight that, in many cases, it would be incorrect to as-
439 sume that units with similar spike shapes recorded on the same electrode in subsequent sessions
440 would correspond to different neurons.

441 We conclude that chronically implanted electrode arrays allow for both sampling of a large set
442 of neurons and detailed analysis of a few long-term units, but different timescales need to be con-
443 sidered when planning experiments. If the objective is to sample the population of neurons across
444 a brain area, experimental sessions could be separated by a month to take advantage of appear-
445 ance and disappearance of neurons on the array. If instead the objective is a detailed analysis of
446 a smaller set of neurons and their interactions, daily recordings for 2-4 weeks are ideal.

447 Features of the spike sorting method

448 We adopted a modular strategy for spike sorting, where individual sessions were processed inde-
449 pendently and could be iteratively merged to form 'supersessions'. In this way, experimenters can
450 perform preanalyses as data are generated and determine receptive fields and tuning properties
451 of neurons to guide stimulus selection as well as monitor recording quality. This modular approach
452 further facilitates excluding particularly noisy segments in individual sessions, which might impair
453 or bias the clustering algorithm.

454 The primary reason for eschewing existing spike sorting methods was a general concern about
455 robustness when stationarity assumptions were not met across recording sessions. This is a known
456 challenge to even cutting-edge algorithms (*Jun et al., 2017a*). We instead chose a simple paramet-
457 ric representation that was designed to be robust to noise and artifacts, which can differ from
458 session to session. Our focus was on characterizing the peak of the depolarization phase using
459 unimodal templates where the SNR would be highest. While spike shapes can be strongly bimodal,
460 depending on the relative position of the electrode and neuron, the shapes for spikes with highest

461 amplitudes near the soma have been shown to be largely unimodal in theoretical studies (*Lindén*
462 *et al., 2011; Quián Quiroga, 2009; Camuñas-Mesa and Quiroga, 2013*). As we recorded spikes on
463 single electrodes and could expect a large number of neurons in the vicinity of an electrode (*Pe-*
464 *dreira et al., 2012*), high amplitude spikes would be easiest to separate from other units. This
465 situation would certainly be different for high-density probes. The process of estimating parame-
466 ters of the spike shapes was essentially an optimization. We would shift a template temporally at
467 sub-sampling resolution and change its width and symmetry to best match a local minimum in the
468 raw voltage traces. In practice, this step was implemented by running the raw data through a large
469 filter bank on a GPU.

470 Our spike sorting approach did not solve the problem of overlapping spikes. However, it greatly
471 reduced the problem as the time interval needed for detection was reduced to the width of the
472 spike and thus, due to zero padding, much smaller than the the width of the templates in the fil-
473 ter bank. In addition, for cases where overlapping spikes exist, we should see them in the shape
474 histograms as somewhat isolated shapes that are a bit wider and of higher amplitude than an ad-
475 jacent cluster. In our data, we did not find evidence for significant numbers of overlapping spikes
476 near isolated clusters. Shape clusters were either nicely separated in the sense that overlapping
477 spikes had at least half an order of magnitude lower amplitudes, or we would be unable to separate
478 clusters in the first place, due to low amplitudes and a large number of sources, with a combined
479 firing rate beyond 100 Hz (as in Figure 3). In the latter case, peak firing rates in single trials in re-
480 sponse to a stimulus can be an order of magnitude higher and we necessarily detect overlapping
481 spikes. Hence, firing rate estimates for low amplitude spikes should be read as a lower bound, pro-
482 viding useful (slightly distorted) information about tuning in sustained responses, while truncating
483 transient responses.

484 In this work, we used the parametric representation of local minima as a spike sorting method.
485 But we could certainly perform spike sorting with an existing method and obtain these parametric
486 representations for spikes in order to subsequently match spike clusters across recording sessions.
487 Likewise, as current sorting techniques are validated with respect to stability over long time frames,
488 it would be straightforward to replace our sorting approach. However, our sorting approach could
489 still be used for fast, online assessments of recording quality, neuronal yield and tuning properties
490 as it does not require manual curation.

491 **Application to data**

492 In many cases, we observed that shape clusters appeared and disappeared gradually over time,
493 such that the observed spike amplitudes were highest around the middle of their lifetime. We
494 could thus have a situation where some shape clusters of a given unit were clearly isolated single
495 unit activity, and others were contaminated (e.g. Figure 7 I). Although this effect means that some
496 of the unit data from ‘supersessions’ is less well-isolated than conventional single-session data, the
497 framework can also be used to estimate the impact of contamination for a given analysis, and
498 hence to determine in a principled manner how high an isolation standard is required.

499 To give an example how such analysis could look like, assume that we have a number of ses-
500 sions (W) where a unit was well-isolated, and some sessions (C), where the same unit was contam-
501 inated with low amplitude spikes from other neurons and some of its spikes were lost due to low
502 amplitudes. We would then pool data from each group (W and C) of sessions to obtain a larger
503 sample size and estimate firing rates and interspike interval histograms.

504 Assuming that low amplitude spikes from other neurons are uncorrelated (alternatively, the
505 interspike interval distribution of low amplitude spikes could be estimated with sufficient data)
506 and uniformly distributed, we would fit the ISI histograms of group C as a linear combination of
507 the ISI histogram of group W and a uniform distribution. The component explained by the uniform
508 distribution could then be translated into an estimate of the spike count for the low amplitude
509 spikes from other neurons (i.e., dividing the rate of the uniform component by spike count of
510 group C and multiply with the total recording duration of group C). To obtain an estimate of the

511 number of spikes missed in group C due to low spike amplitudes, one can multiply the difference in
512 firing rates between group W and C with the total recording duration of group C and add the spike
513 count for the low amplitude spikes determined above. After doing a given analysis separately for
514 groups W and C, one could then compare the results and see how they are affected for a known
515 contamination and signal loss.

516 Furthermore, if one looked into the datasets of group W, one would likely find spikes that are
517 statistically similar to the contaminating spikes in group C, simply by identifying identically shaped
518 spikes at much lower amplitudes. Therefore, it is possible to create surrogate datasets with known
519 contamination (and, by removing spikes, signal loss) and treat them as a model to predict effects
520 on a given analysis. The above analysis would then provide independent data to test this model.

521 Apart from spike clusters, our sorting approach also gives access to low amplitude spikes that
522 do show tuned responses to visual stimulation, but likely arise from a multitude of units with a
523 continuum of corresponding spike shapes (e.g. Figure 3). For the purpose of decoding neural ac-
524 tivity, such low amplitude spikes can be of great value. In fact, results from other groups indicate
525 that lowering the detection threshold increased the performance of a decoder despite losing infor-
526 mation about the neuronal identity (*Trautmann et al., 2019; Kloosterman et al., 2013; Todorova*
527 *et al., 2014*). Our work suggests that we can define a detection threshold (or region of interest)
528 post-hoc, based on responsiveness to stimuli known to drive neural activity. We refer to this ac-
529 tivity as multi-unit hash (MUH), creating a third category alongside with MUA, which should form
530 clusters that are separable from MUH, and SUA which would additionally show a clear refractory
531 period. We need to stress here that MUH is distinct from the 'unsorted spikes' often left behind by
532 most sorting algorithms.

533 In summary, we were able to create 'supersessions' for individual units on a timescale of sev-
534 eral days to a few weeks. This allows for more statistical power than a single session's worth of
535 data can provide, and hence could put the awake marmoset preparation more on par with that of
536 macaques. This is important because the marmoset is also a "pivot species" to richer and more
537 powerful techniques that are more difficult to apply to the macaque. Such supersessions do re-
538 quire reconsidering the design of experiments to handle the comings-and-goings of identified units.
539 Such experiments will likely have a long term structure in which where basic characterization of
540 neural response properties is performed approximately once a week, with the remainder of exper-
541 imental data collection being dedicated to more sophisticated experiments.

542 **Methods and Materials**

543 **Electrophysiology preparation**

544 Two marmosets were with implanted N-Form arrays (Modular Bionics, Berkeley, CA, USA) in area
545 MT (marmoset J) or PPC (marmoset B). Prior to placing the chronically implanted array, we drilled a
546 grid of 9 burr-holes over and surrounding the desired brain area based on stereotaxic coordinates
547 from *Paxinos et al. (2012)*. We performed extracellular recordings using single tungsten electrodes
548 in each burr-hole to fine tune the placement of the array based on the physiological response.
549 The MT array was placed based on high response to direction of motion, while the LIP array was
550 placed based on high eye-movement related activity. A small craniotomy and duratomy were made
551 surrounding the desired area for array placement.

552 The N-form array was mounted on a stereotax arm and manually lowered till tips of the shanks
553 had entered the brain. The brain dimpled slightly, then the tissue relaxed around the implant.
554 The array was then slowly lowered until the baseplate was just above the brain's surface. The
555 array was stabilized and sealed with KwikCast before being closed entirely with dental cement and
556 acrylic. The array connectors were enclosed in a custom 3D-printed box embedded in the acrylic
557 implant.

558 Animal procedures described in this study were approved by the UT Austin Institutional Care
559 and Use Committee (IACUC, Protocol AUP-2017-00170). All of the animals were handled in strict

560 accordance with this protocol.

561 The N-form arrays (Modular Bionics, Berkeley, CA, USA) consisted of a 4x4 grid of electrode
562 shanks, spaced by 400 μm . Each shank was 1.5 mm long and had 4 electrode contacts, one at its
563 tip, and three more at 250 μm , 375 μm and 500 μm distance from the tip. Extracellular signals were
564 recorded at all 64 electrode contacts with sampling rate of 30 kHz, using the OpenEphys recording
565 system (*Siegle et al., 2017*). For marmoset J, seven of the electrode contacts were found damaged
566 after the surgery and ignored for further analyses.

567 **Visual tasks and stimuli**

568 All stimuli were presented using custom MATLAB (Mathworks) code with the Psychophysics Tool-
569 box (*Brainard, 1997*) and a Datapixx I/O box (Vpixx) for precise temporal registration of stimulus,
570 behavioral, and electrophysiological events (*Eastman and Huk, 2012*).

571 Marmosets were trained to fixate a central dot in the presence of peripheral visual stimuli. The
572 animals fixated the dot within a window of 1.5 degree radius for the whole trial to obtain liquid
573 reward in the form of marshmallow juice. If the marmoset broke fixation, the trial was aborted.
574 Fixation was acquired and held for 200 ms before a stimulus appeared.

575 To measure MT receptive fields, we presented a circular cloud of randomly moving dots for
576 350 ms at one of 35 different screen locations during controlled fixation. The diameter of the stim-
577 ulus aperture scaled with the eccentricity of its center.

578 To measure direction tuning, we presented coherent motion in 12 possible directions at a fixed
579 location based on previously measured receptive fields. Each trial contained motion in one direc-
580 tion for a duration of 500 ms.

581 For PPC recordings, marmosets were trained to perform a memory guided saccade task. The
582 animals fixated the central dot while a target dot was briefly flashed at a random location in the pe-
583 riphery. After a delay of 400-1000 ms, the central dot was extinguished and the marmosets received
584 liquid reward for saccades to the remembered location of the target. Memory guided saccades are
585 well known to generate PPC activity in primates (*Andersen et al., 1990*). The task itself was not part
586 of the investigations in this work. We outline it here as context for the behavioral engagement of
587 the animal in the experiments and to emphasize its potential to drive neuronal activity in PPC.

588 On average, recording durations of individual sessions were (26 ± 13) min for marmoset J and
589 (41 ± 12) min for marmoset B.

590 **Pre-processing**

591 We filtered a 60 Hz component out of the raw data for each electrode using a custom made al-
592 gorithm. We also performed common average referencing by subtracting (projections onto) the
593 median of high-pass filtered signals over all electrodes from each channel. We further up-sampled
594 data to 60 kHz before feeding into Kilosort (*Pachitariu et al., 2016*). For this, values between sam-
595 ples were obtained by linear interpolation and values at samples were smoothed with a [1/6 2/3
596 1/6] smoothing kernel to obtain a uniform variance across data points for the case of Gaussian
597 white noise.

598 **Spike sorting**

599 We aimed at jointly sorting spike data from tens of recording sessions (marmoset J: N=154, mar-
600 moset B: N=95) under the following constraints:

- 601 1. Marmosets were head-fixed, but able to move their bodies within the chair, creating tempo-
602 rarily variable amounts of noise in the data.
- 603 2. Electrodes were separated by at least $\geq 125 \mu\text{m}$ and spikes were not generally expected to be
604 seen on multiple electrodes.
- 605 3. We observed only few separable units (0-3) per electrode.
- 606 4. There was no apparent electrode drift within recording sessions.
- 607 5. Spike clusters needed to be matched across recordings.

608 If spike shapes are known, then template matching would be the best way to detect spikes. How-
609 ever, if spikes are to be sorted, information in the raw data needs to be used to separate spike
610 clusters, and especially to separate them from fluctuations in the background noise level and low-
611 amplitude events of neuronal origin. A good sorting algorithm therefore needs to make estimates
612 that are maximally invariant when subjected to noise. Potential issues are:

- 613 1. Baseline estimate: errors could change the match of bimodal templates. This may especially
614 become a problem when the noise level is temporally varied.
- 615 2. Sampling frequency and temporal resolution for peak detection: Misaligned spikes differ in
616 shape. This can be resolved by upsampling the data, but results in longer templates.
- 617 3. Temporally overlapping spikes: Need to be detected and fitted.

618 To address these three issues, we generated a bank of unimodal templates (essentially triangles
619 with a tip rounded off by a cosine function) which varied in phase (to effectively yield 180 kHz sam-
620 pling frequency), width and symmetry (see examples in Figure 8 B), covering a wide range of pos-
621 sible shapes. Each template was normalized to have an energy (sum of squared entries) of one.
622 Using this bank of templates in a template matching strategy reduces baseline errors, temporal
623 misalignment and the chance of fitting overlapping spikes, but does sacrifice some detection power
624 (when compared to using templates generated from the data, about 10% of the signal power).

625 We determined local maxima (in time and width, but global in symmetry to avoid double de-
626 tectations) for the match (dot product) between our templates and the preprocessed voltage traces.
627 In this setting, we were fitting the peak of the depolarization phase of a spike. While an error in
628 the baseline estimate would have an effect on the detected spike power, it would have little effect
629 on both the estimated spike width and symmetry. Temporally overlapping spikes were less likely
630 as the temporal interval for detection was restricted the duration of the depolarization phase (i.e.
631 0.5 ms or less) and a linear combination fitting was not necessary in our recordings. Note that we did
632 not capture the repolarization phase of a spike at all, however, we argue that due to smoothness
633 constraints, the shape of the repolarization phase covaried with its symmetry, and its duration was
634 hard to estimate due to potential drifts in baseline. Matching a large set of potential templates was
635 computationally expensive, but also well suited to run on a GPU. Our implementation ran about
636 twice as long as recording the data for 64 electrodes sampled at 30 kHz. Marginal histograms of
637 shapes obtained for an example recording are shown in Figure 8 C.

638 Spike clusters appear as local density maxima in these histograms. To show that this is indeed
639 the case, we sorted spikes with a widely used spike sorting algorithm (Kilosort, *Pachitariu et al.*
640 (2016)). For that, we used a low threshold for splitting clusters in the Kilosort algorithm and ex-
641 tracted the shapes of the corresponding spikes from our template matching strategy. This allowed
642 us to perform the manual step of merging clusters in an automated procedure, using the Jensen-
643 Shannon divergence between shape histograms as a distance metric.

644 We obtained three dimensional histograms of shape parameters for spikes from each Kilosort
645 cluster (Figure 8 D). We compared Kilosort clusters to clusters obtained by running the watershed
646 algorithm on shape histograms and found a good match for high amplitude clusters (Figure 8 E).
647 The latter clusters were (by construction) better localized in our histograms and we decided to use
648 them instead of Kilosort clusters in the following analyses.

649 Possible extensions

650 We implemented the spike sorting for the case of single, isolated electrodes. An extension to dense
651 arrays is beyond the scope of this article, but we will briefly discuss potential implementation issues
652 here.

- 653 1. Linear arrays/stereotrodes: can be treated as another dimension, like the phase. This just
654 requires one to set a spatial extent of spikes, creating spatially shifted templates. With this
655 method, one could determine maxima at each time frame for each spatial shift, and do a
656 recursive maximization in a second step to obtain spatially isolated maxima.

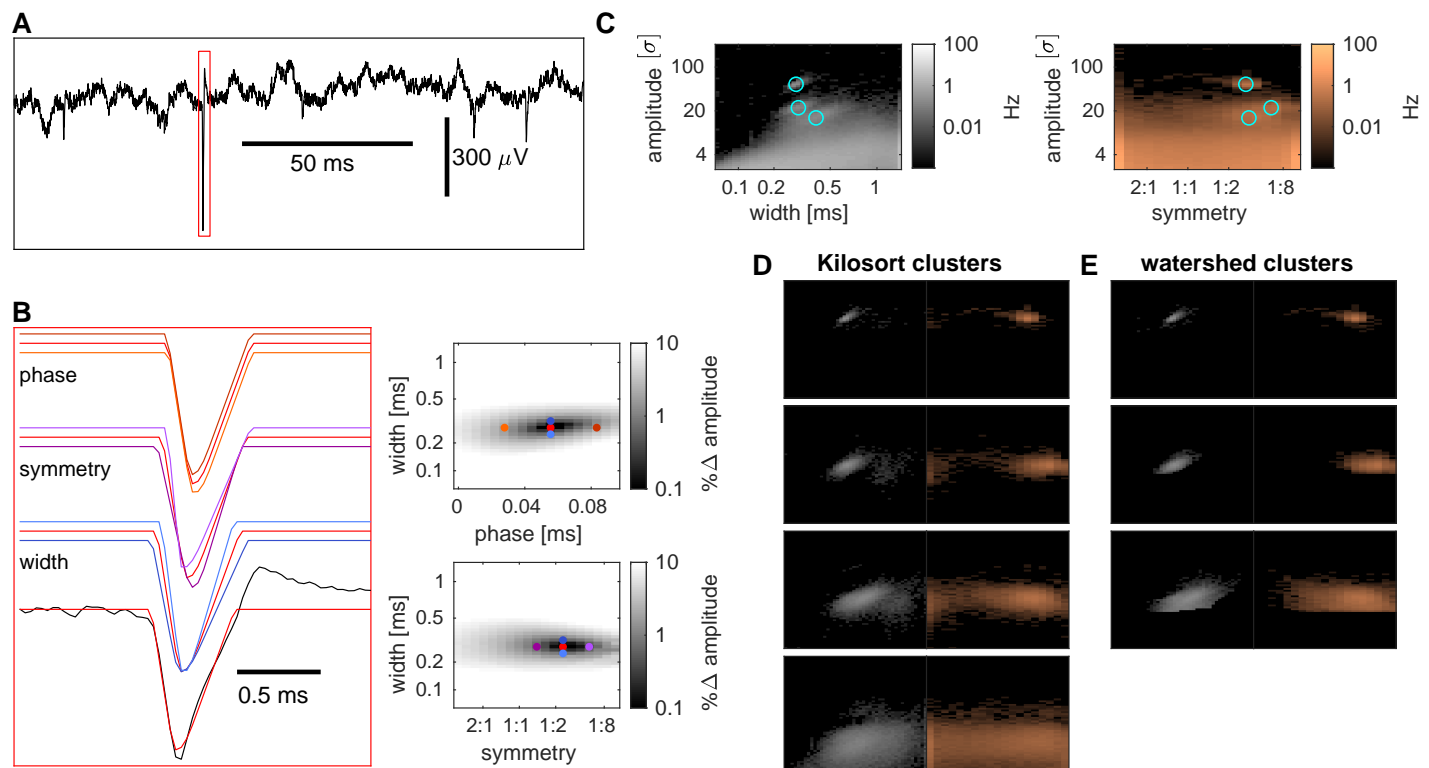


Figure 8. Spike detection and sorting. Raw voltage traces from single electrodes (**A**) are matched in a sliding window to a set of triangular, unimodal templates (examples in **B**, upper left) differing in width, symmetry and phase offset. Local maxima of template - raw trace matches in this parameter space (right plots, red dots) are then detected as putative spikes with a shape characterized by the corresponding width, symmetry and signal power (dot product of template and raw trace). (**C**) Histograms of shapes for an example electrode and recording (marginal distributions). Locations of clusters determined by a watershed algorithm are marked with cyan circles. (**D**) Shapes of events detected by Kilosort on the same electrode, grouped into clusters by an automated procedure. (**E**) Clusters determined by the watershed algorithm (corresponding to the cyan circles in **C**).

657 2. Spatial grids: memory constraints on the GPU will currently require chunking the array into
658 rows of electrodes.

659 Our current implementation does not include a template generation and matching step, poten-
660 tially resulting in suboptimal detection performance. A potential improvement, while still avoiding
661 the baseline issue, could be to generate templates, smooth them with a kernel and generate tem-
662 plate versions with different widths and phases by interpolation. We would need to normalize the
663 templates to unit power and reduce positive (repolarization) parts of the templates (e.g. divide
664 by 2), to reduce a potential baseline effect. Then we would replace the predefined templates of
665 a given cluster (obtained from the watershed algorithm) with these templates, while keeping the
666 other predefined templates as alternative options (for events that do not match a particular tem-
667 plate). Next, we could rerun the detection with the modified set of templates, considering events
668 which are best matching the inserted templates as spikes.

669 Cross-session merges

670 We computed pairwise Jensen-Shannon divergences between existing clusters from the previous
671 2 sessions and clusters from the current session allowing for small shifts in amplitude, width and
672 symmetry for a penalty. Specifically, we did multiply the Jensen-Shannon divergence with the in-
673 verse of Hanning kernels with a half-width of 7 (for amplitude) and 3 (width and symmetry) bins.
674 Each cluster from the current session was then merged with the existing cluster with the smallest
675 Jensen-Shannon divergence if this was below a threshold of $0.3 \ln(2)$, otherwise it was labeled as a

676 new cluster. To allow for slow temporal drifts, the merged cluster was then assigned a shape den-
677 sity equal to the average of the previous and current density (resulting in effective down-weighting
678 of earlier densities).

679 **Motion direction tuning**

680 Using data from all trials across sessions, we determined sensitivity maps (in spike width and am-
681 plitude space) for directional tuning for each electrode in a temporal window from 20-470 ms from
682 stimulus onset. For that, we took spike responses with given amplitude and width, and determined
683 the sensitivity index of direction with the maximum firing rate vs. the opposite direction. That
684 yielded a map of sensitivity indices in dependence of spike shapes which was then thresholded,
685 and split into connected areas exceeding the threshold. The largest of these areas was taken as a
686 mask for the neural response of the electrode. We averaged responses for each of the 12 stimulus
687 directions, temporally filtering with a 20 ms kernel. To see how tuning responses at a given elec-
688 trode site change across sessions, we determined tuning curves for each session. Theoretically, a
689 drift in firing rate or sensitivity could signal a change in coupling between neurons and the elec-
690 trode, eventually caused by z-drift. Likewise, due to the spatial organization of area MT, a change
691 in phase could reflect a lateral movement of the electrode.

692 **Cluster survival**

693 Spike shapes were very similar for a large fraction of clusters. It could be that clusters only ap-
694 peared to last across sessions, but in fact represented multiple different clusters that just hap-
695 pened to have matching shapes. Therefore we wanted to test for a bias in longevity for units with
696 common spike shapes. We computed histograms of amplitudes, widths, symmetry and volume of
697 shape clusters, and the average of these quantities for each better-isolated unit across sessions.
698 We then ranked units according to the local density of shape clusters. A lot of short-lived units had
699 low rank, but this may be a result of detection of low-amplitude units or an increased noise level
700 in some of the recordings. Hence, we determined percentiles (in steps of 10) of the ranks of units
701 surviving for at least 5 sessions. For all units with ranks smaller than a given percentile, we then
702 estimated the conditional probability that a unit was lost in the subsequent session after having
703 survived at least until that session (N). With l_i denoting the measured lifetimes of units, and Θ the
704 Heaviside step function, that probability estimate was

$$p_N = 1 - \frac{\sum_i (l_i - N - 1) \Theta(l_i - N - 1)}{\sum_i (l_i - N) \Theta(l_i - N)}. \quad (1)$$

705 It assumes that after the N -th session, unit losses are described by a Poisson process with a fixed
706 rate.

707 **Receptive fields**

708 Firing rate responses were averaged across sessions and smoothed using a 41 ms Hanning kernel.
709 Maximum responses were obtained for each stimulus condition and visualized. The receptive field
710 was then determined as the region where the spatially interpolated response exceeded a threshold
711 of twice the interquartile range above the median across conditions. Data were insufficient for
712 estimating the size of the receptive field for individual sessions. To visualize the cross-session
713 variation of receptive field locations, we assumed periodic boundary conditions and calculated the
714 circular mean eccentricity and direction (colored circles in Figure 7 A, G). Temporal firing responses
715 of individual sessions (Figure 7 D, J) were smoothed using an 18 ms Hanning kernel.

716 **Acknowledgments**

717 This work was supported by the US BRAIN Initiative (U01 NS094330) to ACH, the University of Texas
718 at Austin (College of Natural Sciences Catalyst Award) to ACH, the National Institute on Drug Abuse
719 (T32 DA018926) to AJL and HCC and the National Eye Institute (T32 EY021462) to AJL.

720 **Competing interests**

721 The authors declare that no competing interests exist.

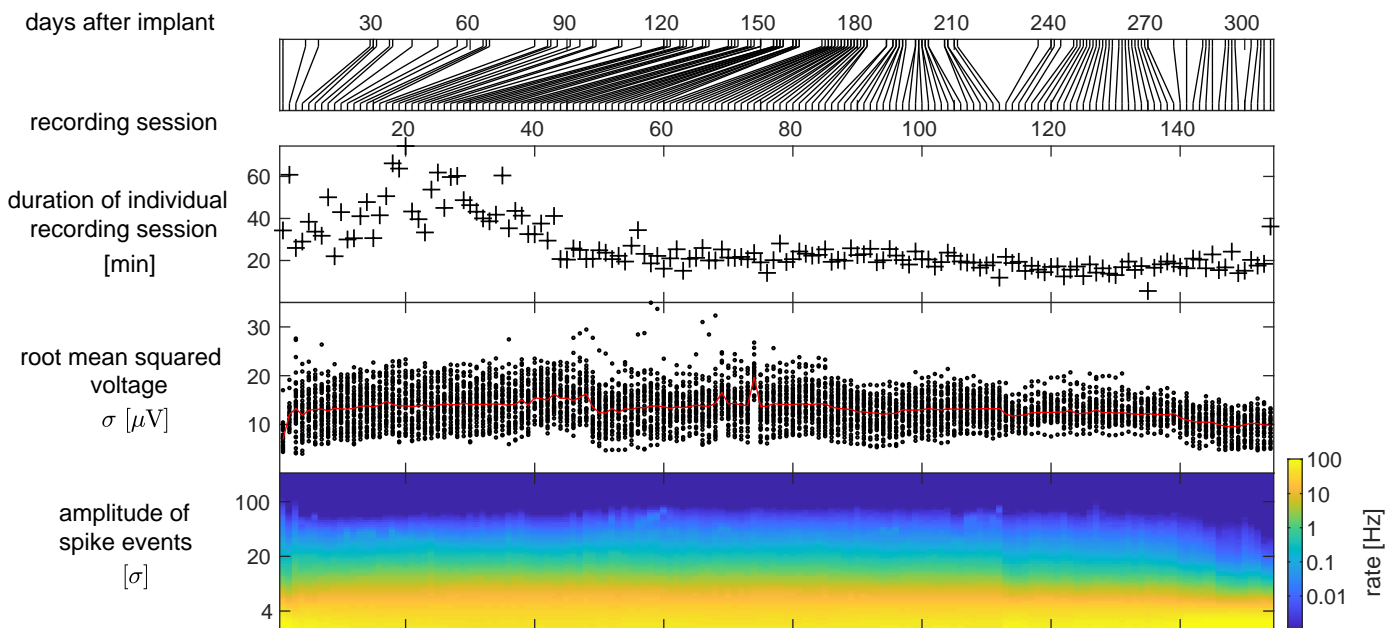
722 **References**

- 723 **Andersen RA**, Bracewell RM, Barash S, Gnadt JW, Fogassi L. Eye position effects on visual, memory, and saccade-
724 related activity in areas LIP and 7a of macaque. *Journal of Neuroscience*. 1990 Apr; 10(4):1176–1196. <https://www.jneurosci.org/content/10/4/1176>, doi: 10.1523/JNEUROSCI.10-04-01176.1990, publisher: Society for
725 Neuroscience Section: Articles.
- 726
- 727 **Brainard DH**. The Psychophysics Toolbox. *Spatial Vision*. 1997 Jan; 10(4):433–436. https://brill.com/view/journals/sv/10/4/article-p433_15.xml, doi: 10.1163/156856897X00357, publisher: Brill Section: Spatial Vision.
- 728
- 729 **Camuñas-Mesa LA**, Quiroga RQ. A Detailed and Fast Model of Extracellular Recordings. *Neural Computation*.
730 2013 Mar; 25(5):1191–1212. https://doi.org/10.1162/NECO_a_00433, doi: 10.1162/NECO_a_00433.
- 731 **Chung JE**, Joo HR, Fan JL, Liu DF, Barnett AH, Chen S, Geaghan-Breiner C, Karlsson MP, Karlsson M, Lee
732 KY, Liang H, Magland JF, Pebbles JA, Tooker AC, Greengard LF, Tolosa VM, Frank LM. High-Density,
733 Long-Lasting, and Multi-region Electrophysiological Recordings Using Polymer Electrode Arrays. *Neu-*
734 *ron*. 2019 Jan; 101(1):21–31.e5. <http://www.sciencedirect.com/science/article/pii/S0896627318309930>, doi:
735 10.1016/j.neuron.2018.11.002.
- 736 **Debnath S**, Prins NW, Pohlmeier E, Mylavarapu R, Geng S, Sanchez JC, Prasad A. Long-term stability of neural
737 signals from microwire arrays implanted in common marmoset motor cortex and striatum. *Biomedical*
738 *Physics & Engineering Express*. 2018 Aug; 4(5):055025. <https://doi.org/10.1088/2057-1976/aada67>, doi:
739 10.1088/2057-1976/aada67.
- 740 **Dhawale AK**, Poddar R, Wolff SB, Normand VA, Kopelowitz E, Ölveczky BP. Automated long-term recording and
741 analysis of neural activity in behaving animals. *eLife*. 2017 Sep; 6:e27702. <https://doi.org/10.7554/eLife.27702>,
742 doi: 10.7554/eLife.27702.
- 743 **Dickey AS**, Suminski A, Amit Y, Hatsopoulos NG. Single-Unit Stability Using Chronically Implanted Multielec-
744 trode Arrays. *Journal of Neurophysiology*. 2009 Aug; 102(2):1331–1339. [https://journals.physiology.org/doi/](https://journals.physiology.org/doi/full/10.1152/jn.90920.2008)
745 [full/10.1152/jn.90920.2008](https://journals.physiology.org/doi/full/10.1152/jn.90920.2008), doi: 10.1152/jn.90920.2008.
- 746 **Eastman KM**, Huk AC. PLDAPS: A Hardware Architecture and Software Toolbox for Neurophysiology Requiring
747 Complex Visual Stimuli and Online Behavioral Control. *Frontiers in Neuroinformatics*. 2012; 6. [https://www.](https://www.frontiersin.org/articles/10.3389/fninf.2012.00001/full)
748 [frontiersin.org/articles/10.3389/fninf.2012.00001/full](https://www.frontiersin.org/articles/10.3389/fninf.2012.00001/full), doi: 10.3389/fninf.2012.00001.
- 749 **Fraser GW**, Schwartz AB. Recording from the same neurons chronically in motor cortex. *Journal of Neuro-*
750 *physiology*. 2011 Dec; 107(7):1970–1978. <https://journals.physiology.org/doi/full/10.1152/jn.01012.2010>, doi:
751 10.1152/jn.01012.2010.
- 752 **Fu TM**, Hong G, Viveros RD, Zhou T, Lieber CM. Highly scalable multichannel mesh electronics for stable chronic
753 brain electrophysiology. *Proceedings of the National Academy of Sciences*. 2017 Nov; 114(47):E10046–
754 E10055. <https://www.pnas.org/content/114/47/E10046>, doi: 10.1073/pnas.1717695114.
- 755 **Fu TM**, Hong G, Zhou T, Schuhmann TG, Viveros RD, Lieber CM. Stable long-term chronic brain mapping at
756 the single-neuron level. *Nature Methods*. 2016 Oct; 13(10):875–882. [https://www.nature.com/articles/nmeth.](https://www.nature.com/articles/nmeth.3969)
757 [3969/](https://www.nature.com/articles/nmeth.3969), doi: 10.1038/nmeth.3969.
- 758 **Huk A**, Bonnen K, He BJ. Beyond Trial-Based Paradigms: Continuous Behavior, Ongoing Neural Activity, and
759 Natural Stimuli. *Journal of Neuroscience*. 2018 Aug; 38(35):7551–7558. [https://www.jneurosci.org/content/38/](https://www.jneurosci.org/content/38/35/7551)
760 [35/7551](https://www.jneurosci.org/content/38/35/7551), doi: 10.1523/JNEUROSCI.1920-17.2018, publisher: Society for Neuroscience Section: TechSights.
- 761 **Jackson A**, Fetz EE. Compact Movable Microwire Array for Long-Term Chronic Unit Recording in Cerebral Cortex
762 of Primates. *Journal of Neurophysiology*. 2007 Nov; 98(5):3109–3118. [https://journals.physiology.org/doi/full/](https://journals.physiology.org/doi/full/10.1152/jn.00569.2007)
763 [10.1152/jn.00569.2007](https://journals.physiology.org/doi/full/10.1152/jn.00569.2007), doi: 10.1152/jn.00569.2007.
- 764 **Jun JJ**, Mitelut C, Lai C, Gratiy SL, Anastassiou CA, Harris TD. Real-time spike sorting platform for high-density
765 extracellular probes with ground-truth validation and drift correction. *bioRxiv*. 2017 Jan; p. 101030. <https://www.biorxiv.org/content/10.1101/101030v2>, doi: 10.1101/101030, publisher: Cold Spring Harbor Laboratory
766 [Section: New Results](https://www.biorxiv.org/content/10.1101/101030v2).
- 767

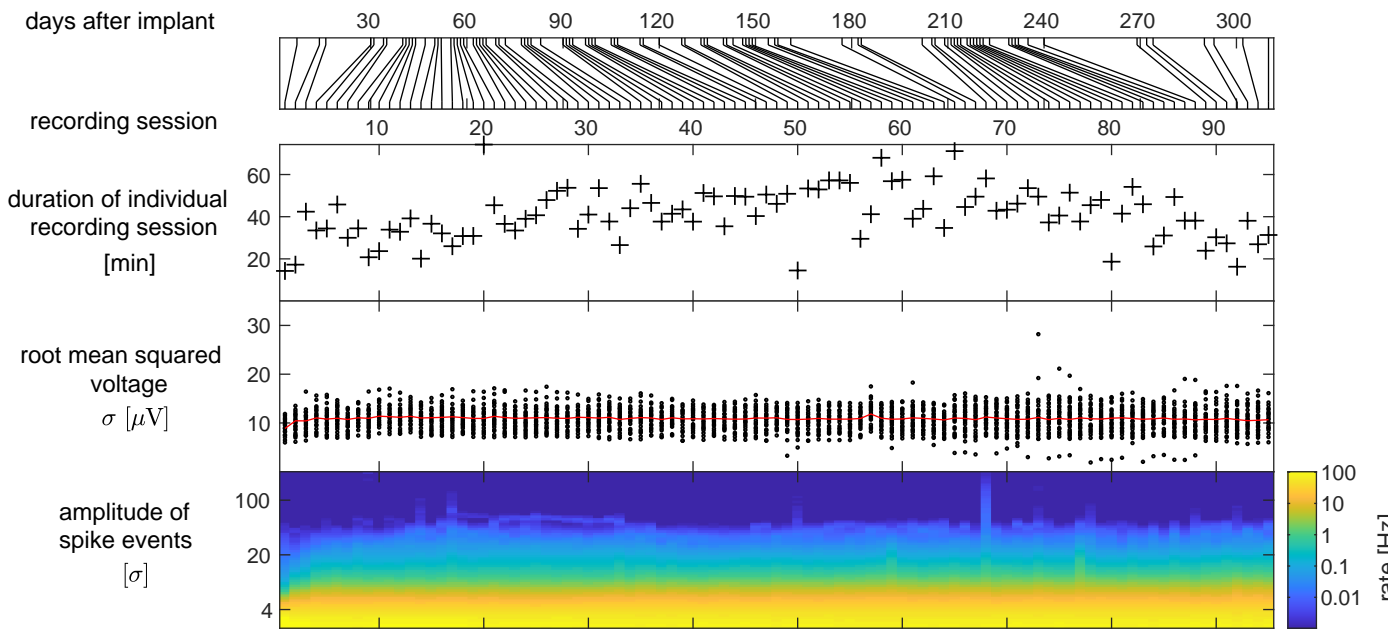
- 768 **Jun JJ**, Steinmetz NA, Siegle JH, Denman DJ, Bauza M, Barbarits B, Lee AK, Anastassiou CA, Andrei A, Aydin
769 C, Barbic M, Blanche TJ, Bonin V, Couto J, Dutta B, Gratiy SL, Gutnisky DA, Häusser M, Karsh B, Ledochow-
770 itsch P, et al. Fully integrated silicon probes for high-density recording of neural activity. *Nature*. 2017 Nov;
771 551(7679):232–236. <https://www.nature.com/articles/nature24636>, doi: 10.1038/nature24636.
- 772 **Kaneko H**, Tamura H, Suzuki SS. Tracking Spike-Amplitude Changes to Improve the Quality of Multi-
773 neuronal Data Analysis. *IEEE Transactions on Biomedical Engineering*. 2007 Feb; 54(2):262–272. doi:
774 [10.1109/TBME.2006.886934](https://doi.org/10.1109/TBME.2006.886934).
- 775 **Karumbaiah L**, Saxena T, Carlson D, Patil K, Patkar R, Gaupp EA, Betancur M, Stanley GB, Carin L, Bel-
776 lamkonda RV. Relationship between intracortical electrode design and chronic recording function. *Biomate-
777 rials*. 2013 Nov; 34(33):8061–8074. <http://www.sciencedirect.com/science/article/pii/S0142961213007989>, doi:
778 [10.1016/j.biomaterials.2013.07.016](https://doi.org/10.1016/j.biomaterials.2013.07.016).
- 779 **Kloosterman F**, Layton SP, Chen Z, Wilson MA. Bayesian decoding using unsorted spikes in the rat hippocam-
780 pus. *Journal of Neurophysiology*. 2013 Oct; 111(1):217–227. <https://journals.physiology.org/doi/full/10.1152/jn.01046.2012>, doi: [10.1152/jn.01046.2012](https://doi.org/10.1152/jn.01046.2012).
- 782 **Knöll J**, Pillow JW, Huk AC. Lawful tracking of visual motion in humans, macaques, and marmosets in a natu-
783 ralistic, continuous, and untrained behavioral context. *Proceedings of the National Academy of Sciences of
784 the United States of America*. 2018; 115(44):E10486–E10494. doi: [10.1073/pnas.1807192115](https://doi.org/10.1073/pnas.1807192115).
- 785 **Linderman MD**, Gilja V, Santhanam G, Afshar A, Ryu S, Meng TH, Shenoy KV. Neural Recording Stability of
786 Chronic Electrode Arrays in Freely Behaving Primates. In: *2006 International Conference of the IEEE Engineering
787 in Medicine and Biology Society*; 2006. p. 4387–4391. doi: [10.1109/IEMBS.2006.260814](https://doi.org/10.1109/IEMBS.2006.260814), ISSN: 1557-170X.
- 788 **Lindén H**, Tetzlaff T, Potjans TC, Pettersen KH, Grün S, Diesmann M, Einevoll GT. Modeling the spatial reach of
789 the LFP. *Neuron*. 2011; 72(5):859–872. doi: [10.1016/j.neuron.2011.11.006](https://doi.org/10.1016/j.neuron.2011.11.006).
- 790 **Nicolelis MAL**, Dimitrov D, Carmena JM, Crist R, Lehew G, Kralik JD, Wise SP. Chronic, multisite, multielec-
791 trode recordings in macaque monkeys. *Proceedings of the National Academy of Sciences*. 2003 Sep;
792 100(19):11041–11046. <https://www.pnas.org/content/100/19/11041>, doi: [10.1073/pnas.1934665100](https://doi.org/10.1073/pnas.1934665100), pub-
793 lisher: National Academy of Sciences Section: Biological Sciences.
- 794 **Okun M**, Lak A, Carandini M, Harris KD. Long Term Recordings with Immobile Silicon Probes in the Mouse Cor-
795 tex. *PLoS ONE*. 2016 Mar; 11(3). <https://www.ncbi.nlm.nih.gov/pmc/articles/PMC4784879/>, doi: [10.1371/jour-
796 nal.pone.0151180](https://doi.org/10.1371/journal.pone.0151180).
- 797 **Pachitariu M**, Steinmetz N, Kadir S, Carandini M, D HK. Kilosort: realtime spike-sorting for extracellular elec-
798 trophysiology with hundreds of channels. *bioRxiv*. 2016 Jun; p. 061481. [https://www.biorxiv.org/content/10.
799 1101/061481v1](https://www.biorxiv.org/content/10.1101/061481v1), doi: [10.1101/061481](https://doi.org/10.1101/061481).
- 800 **Paxinos G**, Watson C, Petrides M, Rosa M, Tokuno H. *The Marmoset Brain in Stereotaxic Coordinates*. El-
801 sevier Academic Press; 2012. <https://espace.curtin.edu.au/handle/20.500.11937/40725>, accepted: 2017-01-
802 30T14:45:05Z.
- 803 **Pedreira C**, Martinez J, Ison MJ, Quian Quiroga R. How many neurons can we see with current spike sorting
804 algorithms? *Journal of Neuroscience Methods*. 2012 Oct; 211(1):58–65. [http://www.sciencedirect.com/science/
805 article/pii/S0165027012002749](http://www.sciencedirect.com/science/article/pii/S0165027012002749), doi: [10.1016/j.jneumeth.2012.07.010](https://doi.org/10.1016/j.jneumeth.2012.07.010).
- 806 **Prodanov D**, Delbeke J. Mechanical and Biological Interactions of Implants with the Brain and Their Impact on
807 Implant Design. *Frontiers in Neuroscience*. 2016; 10. [https://www.frontiersin.org/articles/10.3389/fnins.2016.
808 00011/full](https://www.frontiersin.org/articles/10.3389/fnins.2016.00011/full), doi: [10.3389/fnins.2016.00011](https://doi.org/10.3389/fnins.2016.00011), publisher: Frontiers.
- 809 **Quian Quiroga R**. What is the real shape of extracellular spikes? *Journal of Neuroscience Meth-
810 ods*. 2009 Feb; 177(1):194–198. <http://www.sciencedirect.com/science/article/pii/S0165027008005797>, doi:
811 [10.1016/j.jneumeth.2008.09.033](https://doi.org/10.1016/j.jneumeth.2008.09.033).
- 812 **Rennaker RL**, Street S, Ruyle AM, Sloan AM. A comparison of chronic multi-channel cortical implantation tech-
813 niques: manual versus mechanical insertion. *Journal of Neuroscience Methods*. 2005 Mar; 142(2):169–176.
814 <http://www.sciencedirect.com/science/article/pii/S016502700400305X>, doi: [10.1016/j.jneumeth.2004.08.009](https://doi.org/10.1016/j.jneumeth.2004.08.009).
- 815 **Sedaghat-Nejad E**, Herzfeld DJ, Hage P, Karbasi K, Palin T, Wang X, Shadmehr R. Behavioral training of mar-
816 mosets and electrophysiological recording from the cerebellum. *Journal of Neurophysiology*. 2019 Aug;
817 122(4):1502–1517. <https://journals.physiology.org/doi/full/10.1152/jn.00389.2019>, doi: [10.1152/jn.00389.2019](https://doi.org/10.1152/jn.00389.2019).

- 818 **Siegle JH**, López AC, Patel YA, Abramov K, Ohayon S, Voigts J. Open Ephys: an open-source, plugin-based
819 platform for multichannel electrophysiology. *Journal of Neural Engineering*. 2017 Jun; 14(4):045003. <https://doi.org/10.1088/1741-2552/aa5eea>, doi: 10.1088/1741-2552/aa5eea.
- 821 **Todorova S**, Sadtler P, Batista A, Chase S, Ventura V. To sort or not to sort: the impact of spike-sorting on
822 neural decoding performance. *Journal of Neural Engineering*. 2014 Aug; 11(5):056005. <https://doi.org/10.1088/1741-2560/11/5/056005>, doi: 10.1088/1741-2560/11/5/056005.
- 824 **Trautmann EM**, Stavisky SD, Lahiri S, Ames KC, Kaufman MT, O'Shea DJ, Vyas S, Sun X, Ryu SI, Gan-
825 guli S, Shenoy KV. Accurate Estimation of Neural Population Dynamics without Spike Sorting. *Neu-*
826 *ron*. 2019 Jul; 103(2):292–308.e4. <http://www.sciencedirect.com/science/article/pii/S0896627319304283>, doi:
827 [10.1016/j.neuron.2019.05.003](https://doi.org/10.1016/j.neuron.2019.05.003).
- 828 **Vaidya M**, Dickey A, Best MD, Coles J, Balasubramanian K, Suminski AJ, Hatsopoulos NG. Ultra-long term
829 stability of single units using chronically implanted multielectrode arrays. In: *2014 36th Annual Inter-*
830 *national Conference of the IEEE Engineering in Medicine and Biology Society*; 2014. p. 4872–4875. doi:
831 [10.1109/EMBC.2014.6944715](https://doi.org/10.1109/EMBC.2014.6944715), ISSN: 1558-4615.

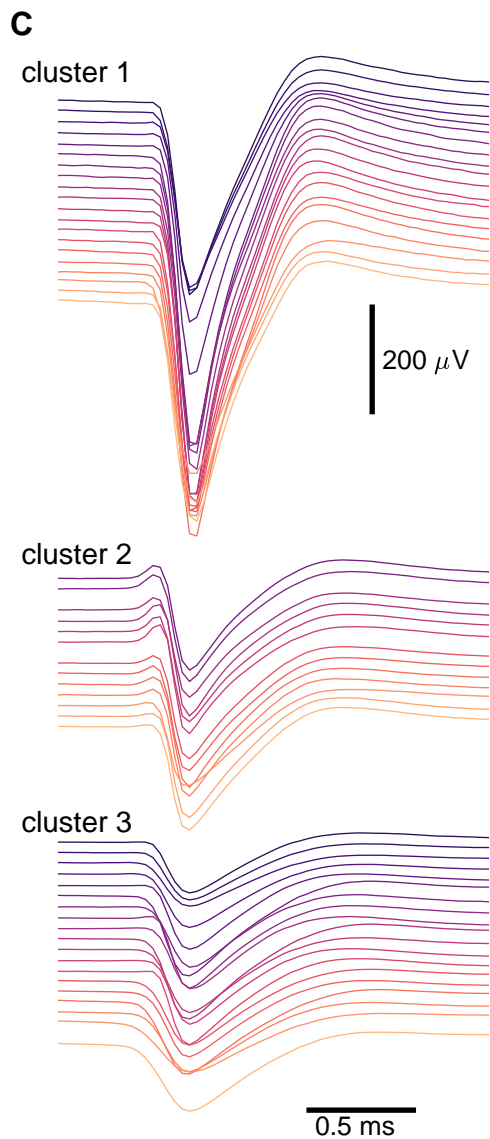
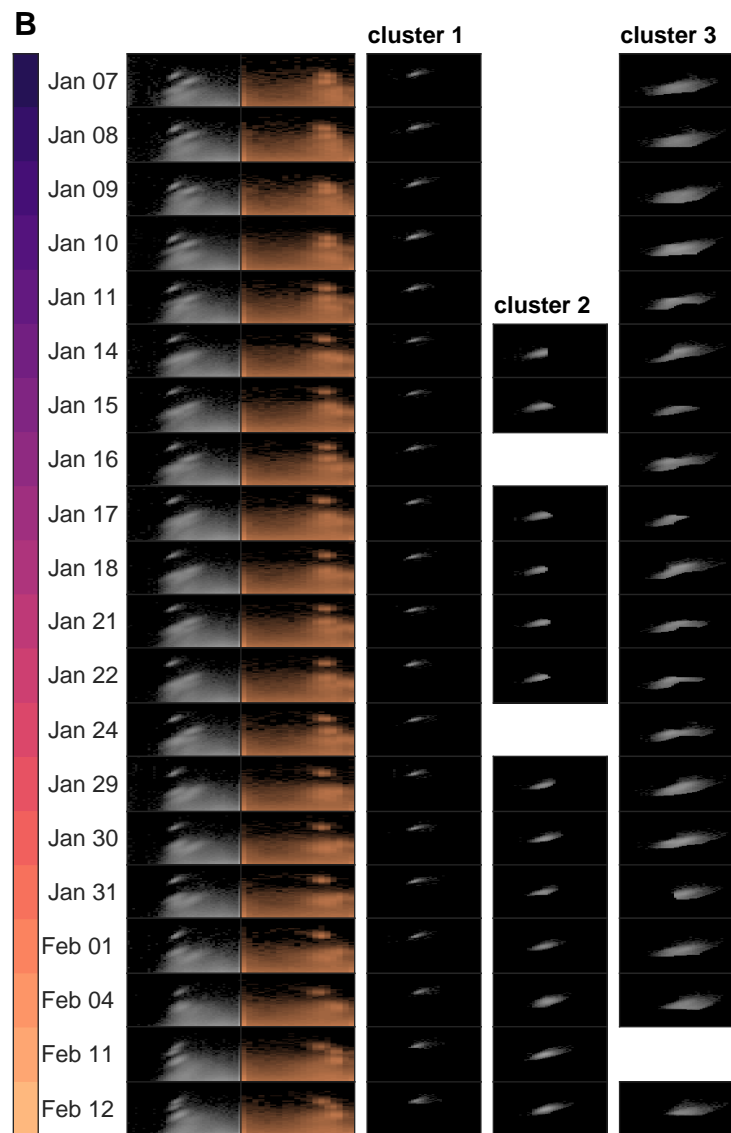
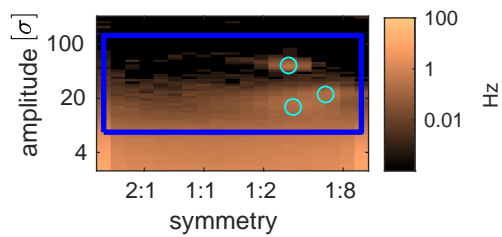
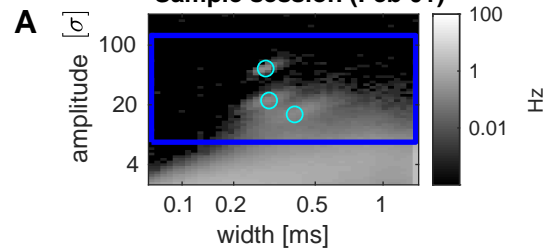
Marmoset J

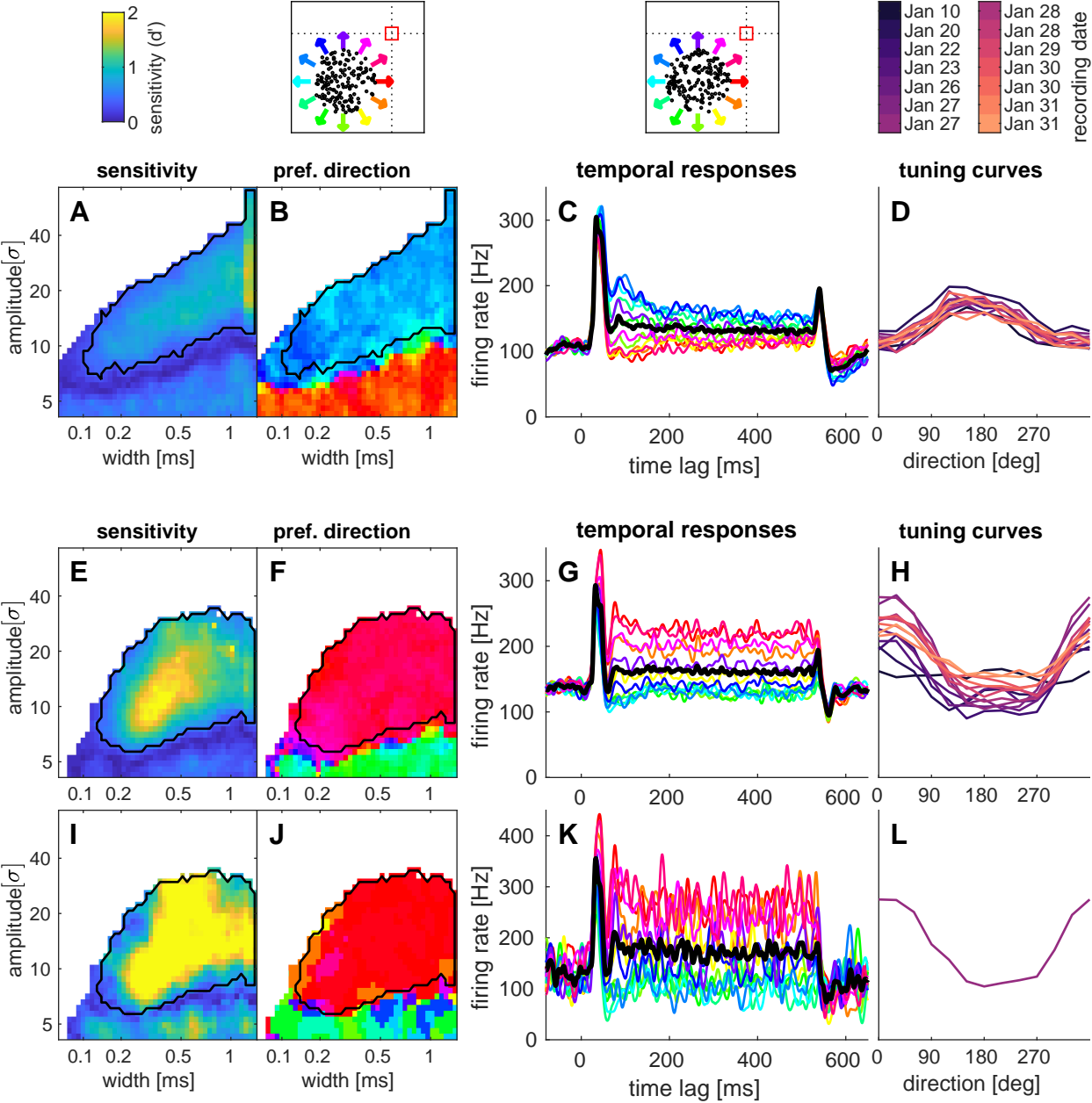


Marmoset B

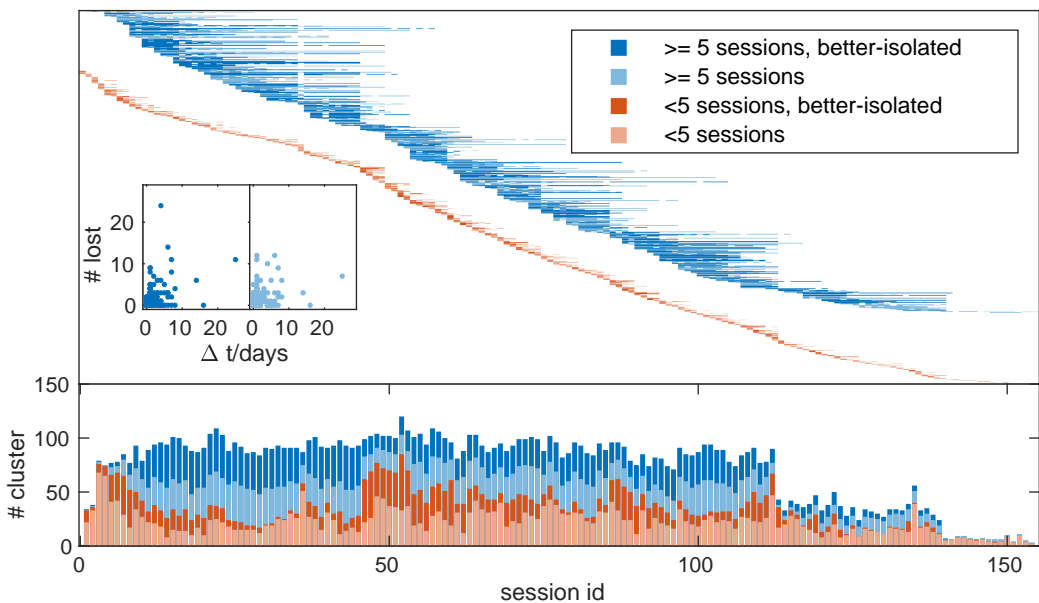


Sample session (Feb 01)

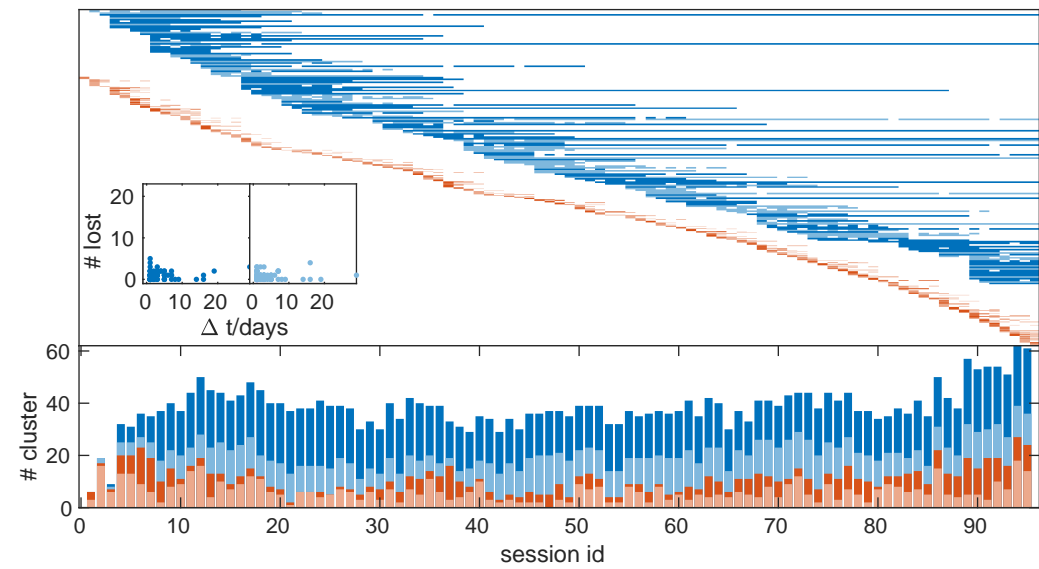




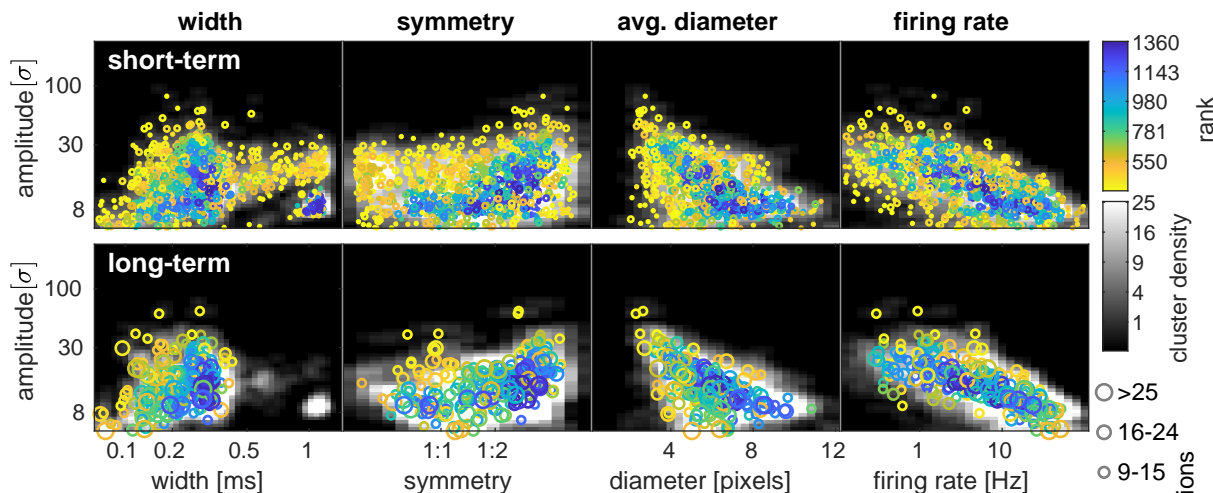
A Marmoset J



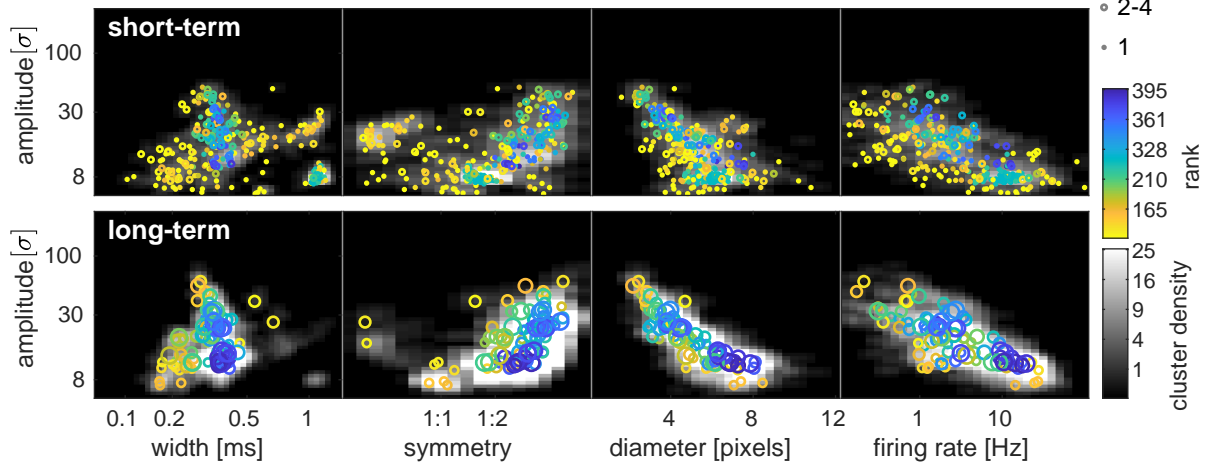
B Marmoset B

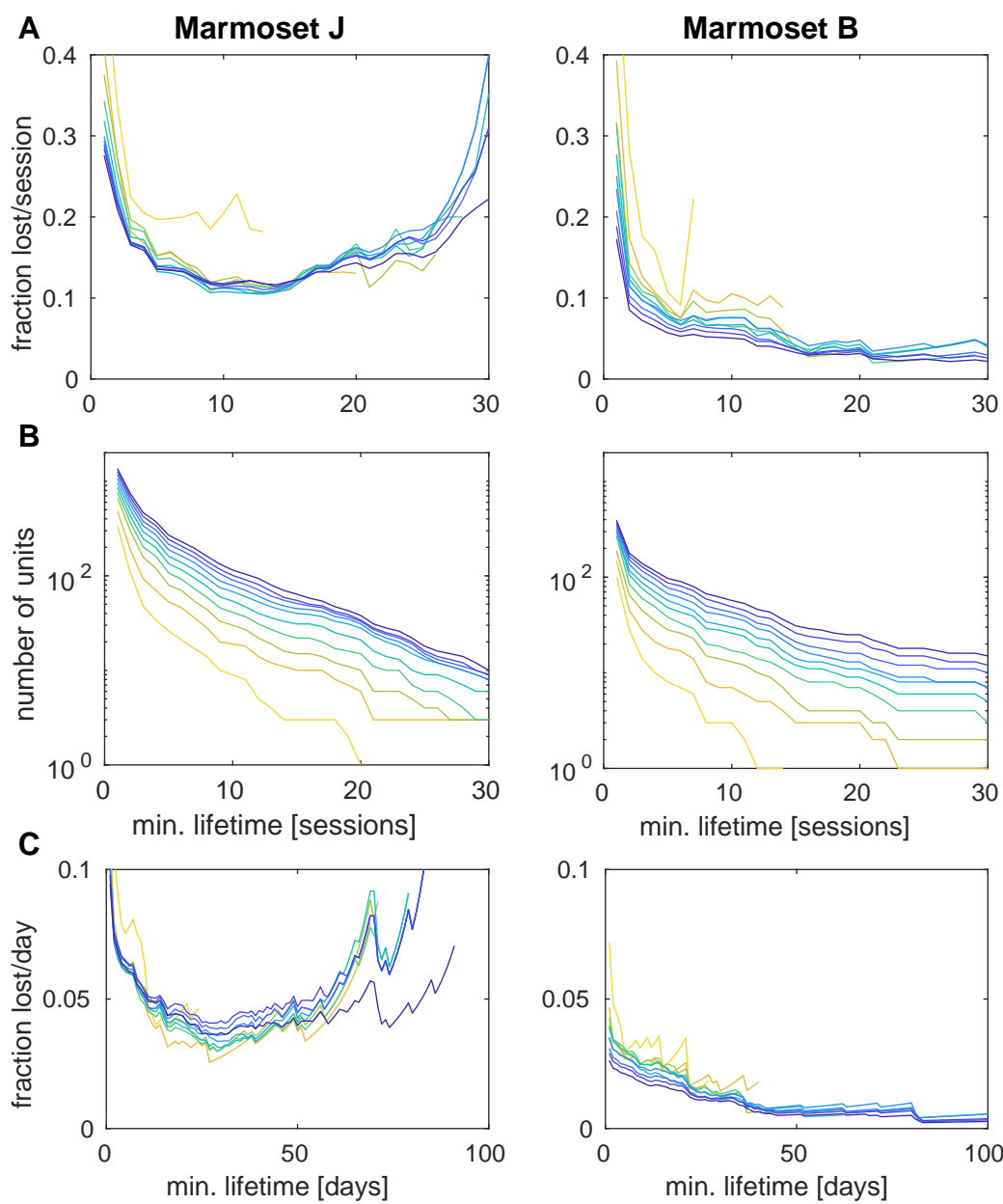


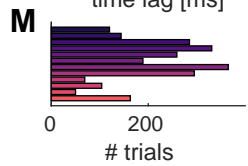
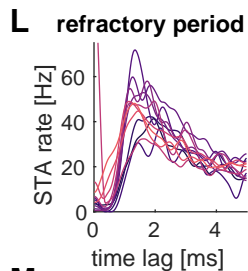
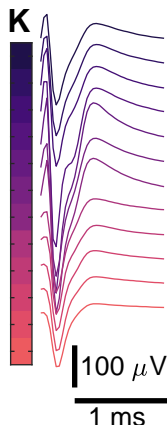
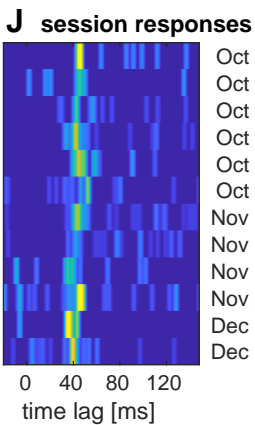
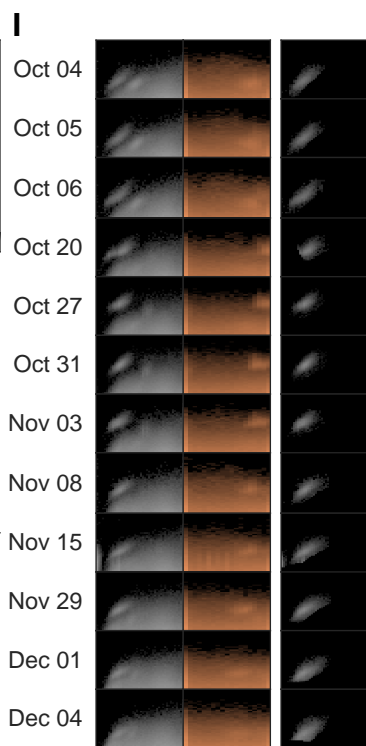
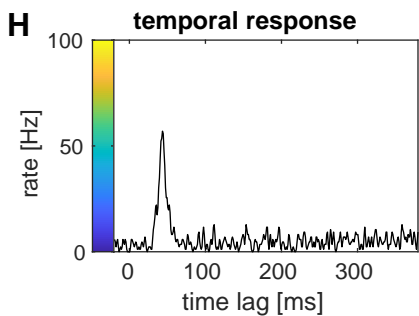
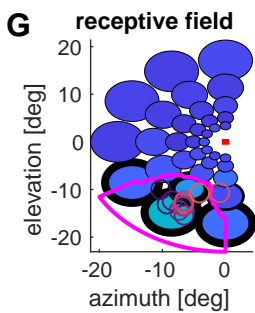
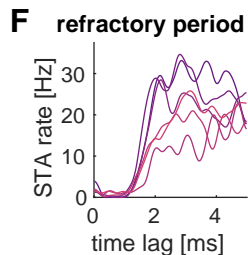
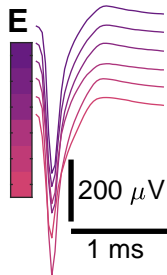
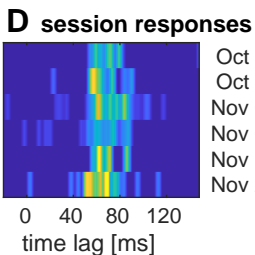
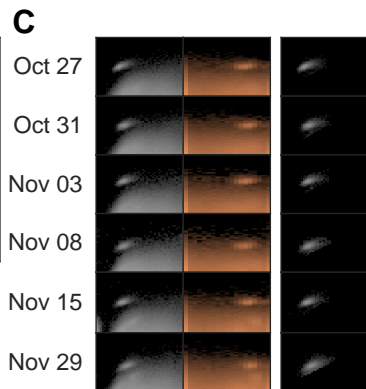
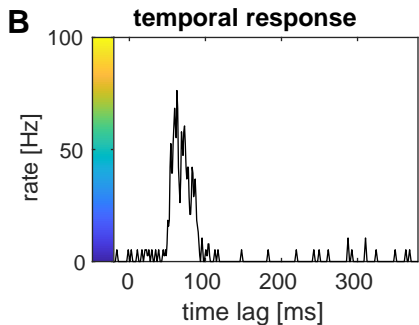
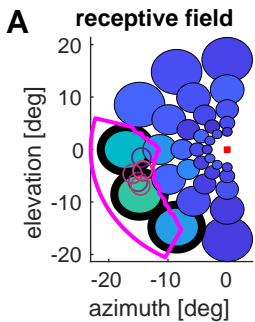
A Marmoset J

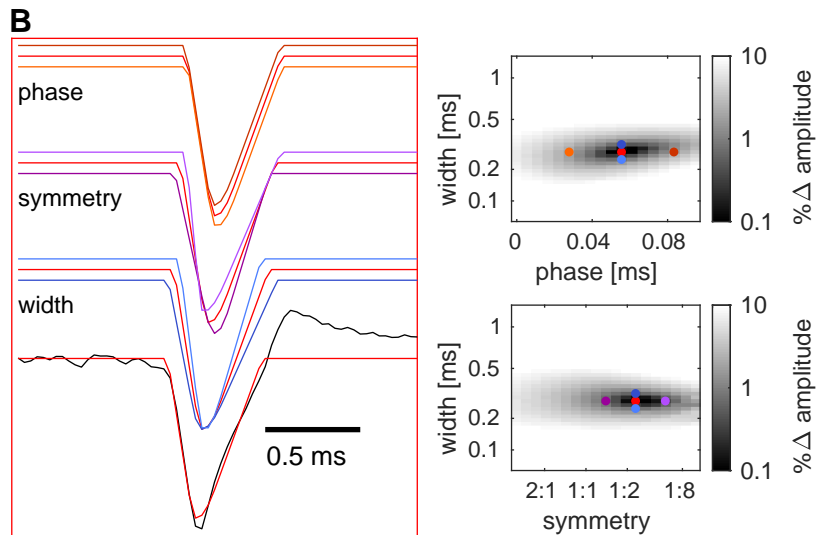
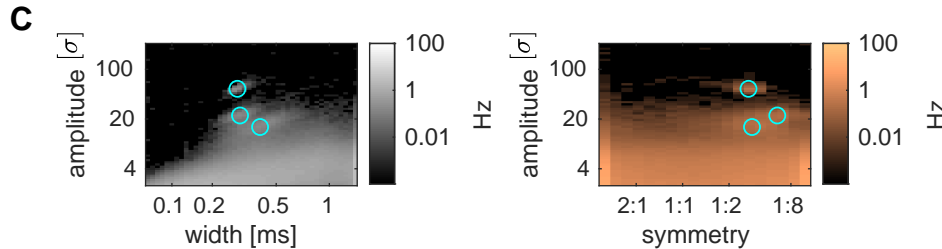
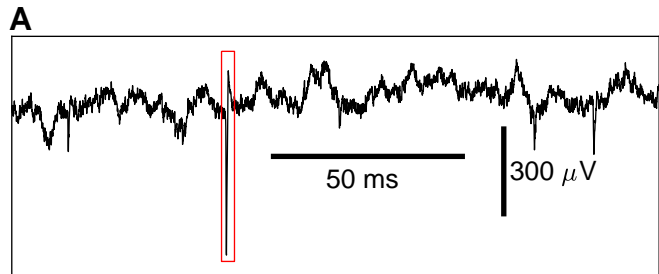


B Marmoset B

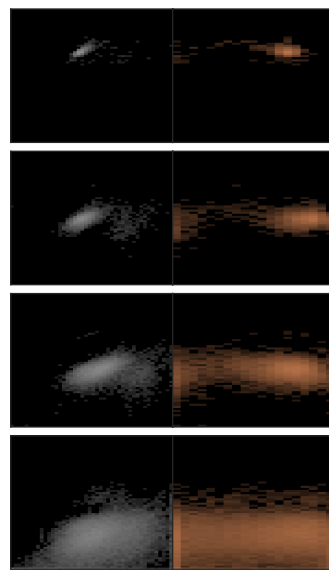








D Kilosort clusters



E watershed clusters

